

DESIGN, CONSTRUCTION, AND TESTING OF AN OPEN
ATMOSPHERIC BOUNDARY LAYER WIND TUNNEL

By

HAROLD SHERWOOD BOUDREAU III

A DISSERTATION PRESENTED TO THE UNDERGRADUATE SCHOOL
OF THE UNIVERSITY OF FLORIDA IN PARTIAL FULFILLMENT
OF THE REQUIREMENTS FOR THE HONOR OF SUMMA CUM LAUDE

UNIVERSITY OF FLORIDA

2009

© 2009 Harold Sherwood Boudreau III

To my friends and family for all their support

TABLE OF CONTENTS

	<u>page</u>
LIST OF TABLES	6
LIST OF FIGURES	7
LIST OF OBJECTS	9
ABSTRACT.....	10
LITERATURE REVIEW	12
WIND TUNNEL LAYOUT	16
Axial Fans.....	18
Diffuser/Plenum.....	19
Diffuser Frictional Loss Coefficient.....	19
Diffuser Pressure Loss.....	20
Diffuser Minimum Length	20
Settling Chamber	20
Mesh Screen Loss Coefficient Equation	21
Contraction	21
Bell and Mehta’s Fifth-Order Contraction Polynomial.....	22
Contraction/Nozzle Loss Coefficient Equation.....	22
Test Section	23
Test Section Loss Coefficient Equation	23
GOVERNING AERODYNAMIC EQUATIONS.....	25
Continuity Equation.....	25
Incompressible Flow Assumption for Low-Speed Applications.....	26
Simplify for Average Two Dimensional Flow Using Eulerian Perspective	26
Bernoulli Equation.....	27
Bernoulli Equation with Added Frictional and Local Losses	27
Pressure Loss Equation Using a Loss Coefficient.....	28
Circuit Energy Loss Equation	28
DIMENSIONAL ANALYSIS	29
Prandtl Number	30
Mach Number	30
Froude Number.....	30
Reynolds Number.....	30
OPEN ABL CALCULATION WORKSHEET	32

CONSTRUCTION.....	38
Axial Fans	38
Minimum Fan Flow Required	38
Diffuser/Plenum.....	39
Settling Chamber	41
Contraction	43
Test Section	44
Completed Wind Tunnel.....	45
MODEL WIND TUNNEL TESTING.....	49
Testing Setup	49
Cobra Probe and TFI Data Acquisition Software.....	50
Testing Method.....	53
Quality Control	55
RESULTS AND RECCOMENDATIONS.....	57
Results.....	57
Recommendations.....	62
Conclusions.....	64
BIOGRAPHICAL SKETCH	68

LIST OF TABLES

<u>Table</u>	<u>page</u>
Table 1-1. Important Events in Wind Engineering.....	12
Table 6-1. ABL Wind Tunnel Materials, Costs, and Suppliers.....	48
Table 8-1. Model ABL Wind tunnel Testing Results.....	58

LIST OF FIGURES

<u>Figure</u>	<u>page</u>
Figure 1-1. United States Subsonic Wind tunnels	14
Figure 2-1. Main Wind tunnel Layouts. A) Closed Loop System, B) Open System.....	16
Figure 2-2. Overall ABL Wind tunnel Layout A) Side View, B) Plan View, C) Cross Section A-A	18
Figure 3-1. Continuity Equation Figure.....	26
Figure 5-1. Open ABL Calculation Worksheet: “Givens” Page.....	33
Figure 5-2. Open ABL Calculation Worksheet: “Calculations” Page 1 of 5.....	33
Figure 5-4. Open ABL Calculation Worksheet: Plan View	36
Figure 6-1. 26 inch High Velocity Patterson Fan	39
Figure 6-2. 26 inch High Velocity Fan Air Flow Pattern	39
Figure 6-3. Plenum Construction Template.....	41
Figure 6-4. Plenum Construction: A) Attachment with Rivets and Liquid Nails B) Weather stripping with Silicone Caulking and Foil Tape	41
Figure 6-5. Completed Settling Chamber with Honeycomb and Mesh Screens	43
Figure 6-6. Contraction Template.....	44
Figure 6-7. Contraction Construction: A) Side Construction B) Completed Construction.....	44
Figure 6-8. Test Section Construction: A) Caulking Interior Corners B) Reinforced Support and Tie Down.....	45
Figure 6-9. Completed Wind Tunnel	47
Figure 7-1. Cobra Probe Testing Setup: A) Computer B) Setup Probe Close-Up	49
Figure 7-2. Cobra Probe Layout	50
Figure 7-3. Cobra Probe Axis System	51
Figure 7-4. Cobra Probe TFI Device Control Data Acquisition Software	53

Figure 7-5. ABL Wind Tunnel Testing Locations: A) Longitudinal Locations B) Vertical Locations.....	54
Figure 8-1. ABL Test Section Mean Wind Speed: A) Overall Mean Wind Speed B) Mean Wind Speed in X-Direction C) Mean Wind Speed in Y-Direction D) Mean Wind Speed in Z-Direction.....	59
Figure 8-2. ABL Test Section Mean Turbulence: A) Overall Mean Turbulence B) Mean Turbulence in X-Direction C) Mean Turbulence in Y-Direction D) Mean Turbulence in Z-Direction.....	61
Figure 8-3. ABL Velocity Profile at End of Test Section.....	62

LIST OF OBJECTS

<u>Object</u>	<u>page</u>
Object 5-1. Open ABL Calculation Worksheet (.xls file 155KB).....	37

Abstract of Dissertation Presented to the Undergraduate School
of the University of Florida in Partial Fulfillment of the
Requirements for the Honor of Summa Cum Laude

DESIGN, CONSTRUCTION, AND TESTING OF AN OPEN
ATMOSPHERIC BOUNDARY LAYER WIND TUNNEL

By

Harold Sherwood Boudreau III

May 2009

Chair: David Prevatt

Major: Bachelor of Science in Civil Engineering

Hurricane winds destroy building and structures that house businesses and residents around the globe. More than half of the United States' population lives in coastal counties, and as that proportion continues to rise hurricane research will increase in importance well into the future.

In order to better design building, structural engineers need methods to estimate the damaging wind loads caused by extreme hurricane winds. One of the most common methods is by using wind tunnels. This research project aims to establish appropriate performance criteria for a full-scale open atmospheric boundary layer (ABL) wind tunnel that can replicate various quasi-steady and turbulent flow states on low-rise building models up to 1:25 scale. In general ABL wind tunnels can be used to research wind effects on low-rise and high-rise structures, curtain wall testing, air quality and pollutant dispersion, snow dispersion, and wind infiltration and exfiltration. The wind tunnel can create very accurate structural modeling and be more representative of actual failure modes and fatigue. Better understanding the failure modes and roof pressures of low-rise structures could lead to advancements in retro-fitting current buildings and specific joint reinforcement for new construction.

Theoretical equations as well as empirical models from current wind tunnel papers will be used to create a viable wind tunnel design. After reviewing the current literature, a scale model

will be created to test the validity of the proposed wind tunnel design. A method for testing the wind tunnel head loss and pressure distribution will be developed in an attempt to compare the actual results with the anticipated results from the literature research. The culmination of the test result comparison will be recommendations for a full scale ABL wind tunnel.

CHAPTER 1

LITERATURE REVIEW

Wind engineering is a field that has been evolving over centuries. The first step in wind engineering was over 350 years ago when Torricelli invented the barometer to measure air pressure (Cochran 4). There have been many changes over the years, but at its core wind engineering is based on using measurements of actual wind flows to predict the forces transferred to engineered structures and machines. Dr. Leighton Cochran from Cermak Peterka Peterson, Inc. created a table listing some of the important events that have led to wind engineering as it is known today, See Table 1-1.

Year	Researcher	Event
1643	Torricelli	Invents barometer
1687	Newton	Defines viscosity, laws of motion, calculus, Principia
1738	Bernoulli	Defines conservation of energy in fluids, Hydrodynamica
1755	Euler	Form inviscid equations of fluid motion
1806	Beaufort	Defines wind-speed in term of visible effects
1836		Collapse of Brighton Chain Pier by oscillatory motion
1845	Stokes	Formulates Navier-Stokes equations of fluid motion
1846	Robinson	Invents cup anemometer
1879		Collapse of the Tay Bridge in Scotland
1883	Reynolds	Dimensionless parameter that indicates onset of turbulence
1888	Dines	Invents pressure tube anemometer
1904	Prandtl	Develops the boundary-layer concept
1912	von Kármán	Identifies vortex shedding in wakes
1914	King	Defines equation for cooling of hot cylinders
1928	Fisher & Tippet	Develop theory of extreme values
1934		Highest measured gust at Mt. Washington (370 km/h)
1935	Taylor	Develops statistical theory of turbulence
1940	Rathbun	Collected full-scale deflections on the Empire State Building
1940		Collapse of Tacoma Narrows Bridge by oscillatory motion
1954	Cermak	Builds first large boundary-layer wind tunnel
1954	Jensen	Formulates model scaling laws
1957	Van der Hoven	Compiles wide frequency range spectrum of the wind
1958	Cermak	Reynolds number independence in modeling boundary layer
1961	Davenport	Develops statistical concepts to wind loadings
1963		1st International Conference on Wind Effects on Buildings
1964	Cermak & Davenport	First major building study in a boundary-layer wind tunnel – The World Trade Center Twin Towers in New York City
1965		Collapse of three cooling towers at Ferrybridge
1970		Term “Wind Engineering” coined
1974	Eaton & Mayne	Aylesbury House study in Britain
1976	Deaves & Harris	Develop mathematical model for strong winds
1979	Melbourne	Shows importance of turbulence in bluff-body aerodynamics
1986		Amarube Tekkyo rail bridge disaster in Japan
1984	Holmes	Defines wind-tunnel pressure tubing response characteristics
1987	Mehta	Texas Tech University Experimental Building is built
1988	Robertson & Glass	Silsoe Structures Building is built
1992	Murakami	1st Computational Wind Engineering Symposium, Tokyo

Sources: Aynsley Vickery and Melbourne [1977], Britannica [1968], Cermak [1975], Melbourne [1979], Cochran [1992], Cook [1985], Holmes [1984], McWhirter [1986], Takagi [1992] and Timoshenko [1953]

Table 1-1. Important Events in Wind Engineering

A large portion of wind engineering today relies directly or indirectly on wind tunnels. Wind tunnels are used for a variety of different reasons such as their ability to test prototypes early in design cycles, or because of their ability to record a large amount of data (Barlow 19). Probably the most important aspect of wind tunnels is their ability to accurately recreate the full complexity of full fluid flow (Barlow 19). Wind tunnels are especially used when testing new designs and materials, such as the World Trade Center Twin Towers noted in Table 1-1; this is because of their ability to simultaneously account for wind interactions, as well as material and geometric properties. When testing new materials and designs many times these interactions and properties are not fully known, limiting the use of finite element analysis software.

Another reason why subsonic wind tunnel research has become so prevalent is the number of available wind tunnels both public and private. Figure 1-1 shows some of the many subsonic wind tunnels available here in the United States (The Worthey Connection). Like most engineering projects each wind tunnel is unique and designed for a specific purpose, giving each wind tunnel different sizes, speeds, and Reynolds Numbers.

Organization	Wind Tunnel	Test Section (ft)	Speed Range (Mach No.)	Reynolds No. (per ft x 10 ⁶)
NASA Ames Research Center	80 X 120 ft	80 x 120	0 to 100 kts	0 - 1.2
	40 X 80 ft	40 x 80 x 80	0 to 300 kts	0 - 3
	12 ft Pressure Tunnel	11.3 x 11.3 x 28	0.05 - 0.55	0.1 - 12
NASA Langley Research Center	14 X 22 Foot Subsonic Tunnel	14.5 x 21.75 x 50	0 to 0.3	0 to 2.1
	12 foot Low Speed Tunnel	12 ft x 15 ft	0 to 77 ft/sec	0 to 0.5
	Low-Turbulence Pressure Tunnel (LTPT)	7.5 x 3 x 7.5	0.05 - 0.5	0.4 - 15.
	20-foot Vertical Spin Tunnel	20 dia, 25 H	0 to 85 ft/sec	0.0 to 0.15
NASA Glenn Research Center	9 X 15 ft	9 x 15	0 - 0.2	0 - 1.4
	Icing Research Tunnel	6 x 9	0 - 0.5	3.3
US Air Force Research Laboratories	SARL	10 x 7	0.20 - 0.50	
	Vertical Wind Tunnel	12 x 15	0 - 150 ft/sec	0 - 0.91
Naval Surface Warfare Center, Carderock Division	Subsonic	8 x 10	20 - 275 ft/sec	1.75
US Army Aeromechanics Laboratory	Army Aeromechanics	7 x 10	0 - 0.33	0 - 2.1
The Boeing Company	20 X 20	20 x 20	0 - 215 knots 0 - 100 knots (open-jet)	0 - 2.3
	BRAIT	5 x 8 4 x 6 (w/inserts)	0 - 150 knots (5x8) 0 - 250 knots (4x6)	
	9 x 9 Subsonic Propulsion Tunnel	9 x 9	0 - 200 knots	
Lockheed Martin	LSWT # 1 & 2	30 x 26 (#1) 16 x 23 (#2)	14 - 146 ft/sec (#1) 29 - 293 ft/sec (#2)	0 - 1 0 - 2
	8 X 12	8 x 12	0 - 293 ft/sec	0 - 1.7
	IWT	4 x 2.5	88 - 308 ft/sec	0 - 2
Allied Aerospace Industries - Micro Craft	LSWT	8 x 12	0 - 0.37	0 - 2.5
Northrop Grumman	Research	2.5 x 3.5	Max Q = 60 psf	1.7
	7 X 10	7 x 10	Mach = 0 to 0.36	1.8
United Technologies	Large Subsonic WT	8' Octagonal x 16' long	Mach = 0 to 0.90	4.5
		10 x 15 x 31	Mach = 0 to 0.45	2.6
	Acoustic Research Tunnel	18' Octagonal x 40' long	Mach = 0 to 0.26	1.6
		5' Diameter	Up to Mach = 0.65	4.6
	Pilot Wind Tunnel	50" Diameter x 8' long	Up to Mach = 0.35	4.6
		4 x 6 x 8	Mach = 0.12	0.9
Allen G. Davenport Wind Engineering Group	BLWT 1	7.2' wide x 6.45' high x 99' long	Mach = 0 to 0.045	
	BLWT 2	15' wide x 12' high x 156' long	Mach = 0 to 0.030	
Georgia Institute of Technology	7 X 9 ft	7 x 9	0 - 0.22	0 - 1.6
	Low Turbulence	3.5 x 3.5	73 ft/sec	0.5
Massachusetts Institute of Technology	Wright Brothers	7.5 x 10 Elliptical	Up to 0.36 @ 0.25 bar	Up to 2.25 @ 1.5 bar
University of Maryland	Glenn L. Martin	7.75 x 11.04	0.0 - 0.3	N/A
Old Dominion University	Langley Full Scale Tunnel	30 x 60	38 - 132 ft/sec	1
Texas A&M University	7 X 10 ft	7 x 10	0 - 0.25	0 - 1.9
Virginia Polytechnic Institute	Stability Wind Tunnel	6 x 6	0 - 275 ft/sec	1.5
University of Florida	anechoic wind tunnel	2.43 x 3.67 x 6.00 ft	0 - 76 m/s	3 - 4
University of Washington	Kirsten Wind Tunnel	8 x 12	0 - 302 ft/sec	0 - 1.8
Wichita State University	Beech Wind Tunnel	7 x 10	0 - 264 ft/sec	0 - 1.5

Figure 1-1. United States Subsonic Wind tunnels

It is customary to construct a model prototype wind tunnel before the full-scale wind tunnel to work out design problems early in the design cycle. In addition to being prototypes for the final wind tunnel design these model wind tunnels have been shown to produce very accurate flow modeling results such as the 24th scale tunnel used for National Aeronautics and Space Administration's (NASA) Vertical /Short Take-Off Landing (V/STOL) wind tunnel and the 10th scale used for the German-Dutch Wind Tunnel (DNW) (Barna 4). In his paper Barna even found very accurate results in his testing a 60th scale model tunnel. As part of this project a 10th scale

wind tunnel will be constructed. This model wind tunnel will be used to test the settling chamber layout, honeycomb design, contraction design, and test section dimensions. The testing for this design will focus on flow stability and uniformity in the test section as well as the maximum attainable wind speed. The design considerations and layout for this ABL wind tunnel are discussed in Chapter 2.

CHAPTER 2

WIND TUNNEL LAYOUT

Two main layouts considered for this wind tunnel are closed loop and open. In a closed loop system the air is re-circulated, see Figure 2-1A; in an open system the air is used only once and released back into the surroundings, see Figure 2-1B (Tomia).

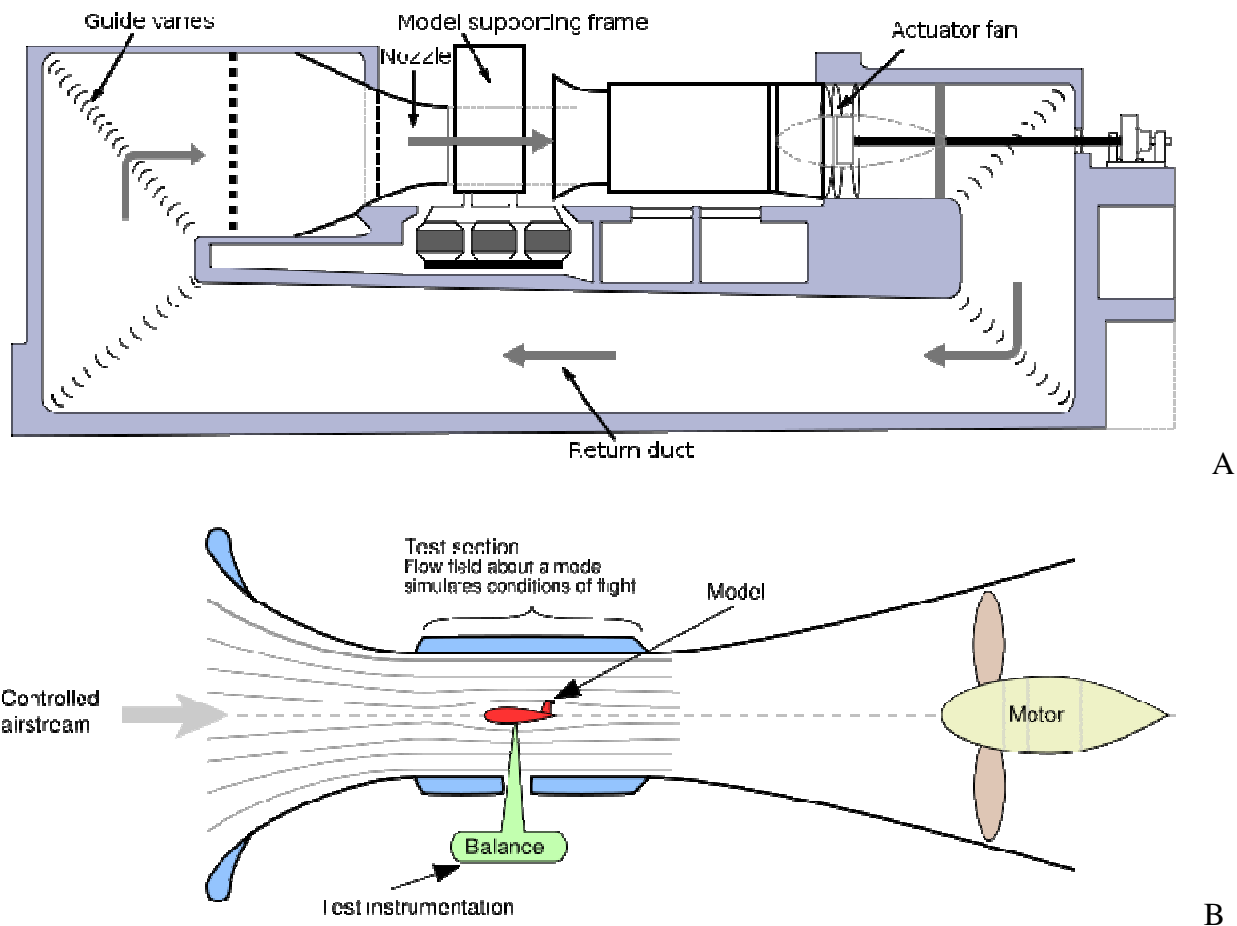


Figure 2-1. Main Wind tunnel Layouts. A) Closed Loop System, B) Open System

Both designs have their own advantages and disadvantages. The open system has a much lower capital investment, but requires larger more powerful fans. The closed loop system requires a larger capital investment, but uses less powerful fans because the loop maintains the net circuit pressure (Boyle 31). To recoup the initial capital investment of a closed system the

wind tunnel would have to be utilized five or six days a week for two or three shifts (Barlow 27). While the wind tunnel is expected to be utilized by multiple departments, it is not expected to meet the high utilization requirements to make it financially beneficial to use the closed system. The open system has the problem with excessive noise production limiting the hours that it can be run, however since this wind tunnel is not expected to require utilization late at night this should not be a problem (Barlow 27). The closed system can be fitted with heat exchangers so that it can be used for experiments that are temperature sensitive or require thermal modeling. Because most of the anticipated research would not be temperature sensitive or need thermal modeling it would be suggested to use the open circuit design to save on total costs. For the research that is temperature sensitive the additional cost of running heat exchangers would still be minimal compared to the additional capital cost of constructing the closed loop system. In addition to the cost savings, one of the greatest benefits of using the open system is that it is capable of environmental modeling such as snow modeling, pollution dispersion, and erosion analysis, making the system very versatile. Since the main purpose of this wind tunnel will be for hurricane testing where the models may be tested to failure an open wind tunnel is preferable because it is much less susceptible to damage from model debris after failure (Barlow 102). Finally, by using an open wind tunnel design smoke can be used for instantaneous flow visualization around structures.

The main components of the proposed wind tunnel in order from intake to outlet are the axial fan, plenum, settling chamber, contraction, and test section. This layout with dimensions specific to this project is shown in Figure 2-2.

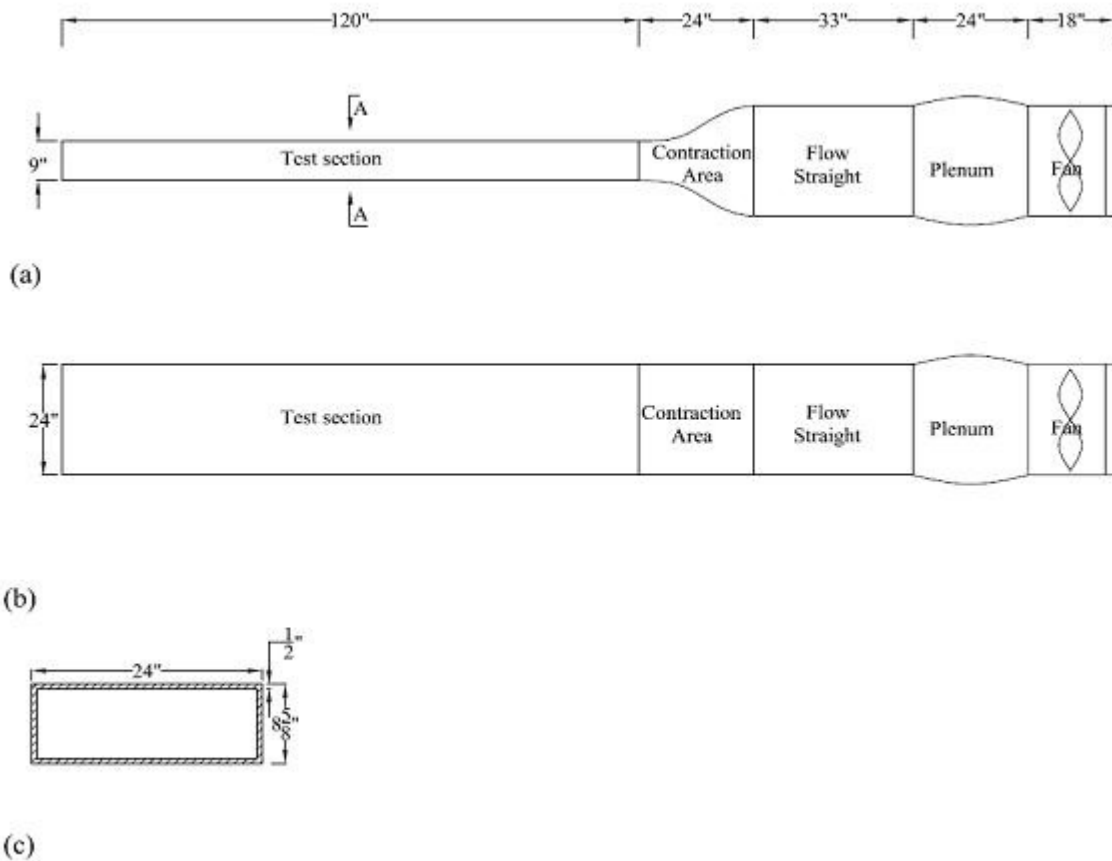


Figure 2-2. Overall ABL Wind tunnel Layout A) Side View, B) Plan View, C) Cross Section A-A

Axial Fans

There are many different fans that can be used in the wind tunnel to achieve the required dimensional similarity. Electric axial fans were selected for their low cost and efficiency in producing high wind velocities. The disadvantage of using axial fans is they impart a small amount of tangential velocity that has to be rectified with counter-rotational vanes and/or additional flow conditioners. The cost of the added flow conditioning for the axial fan is much less than the cost of blowers, which produce a more uniform velocity distribution. Axial fan speeds can be regulated either by adjusting the rotational speed or the pitch of the blades. It is suggested that choosing a fan with adjustable pitch is preferred to fixed blades because it allows

for a larger range of stable flow conditions and reduces stalling problems (Barlow 103). For this project however variable pitch fans for the model would be prohibitively expensive, so fixed blade axial fan were used; for the full scale wind tunnel it would be best to invest in variable pitch blades to enable the most precise adjustments. The axial fans selected are electric driven. These electric fans have the advantage over their combustion driven counterparts because they have less fluctuations, lower operating costs, and have shown to be more reliable in practice (Patterson Fan Inc.).

Diffuser/Plenum

The wind tunnel diffuser/plenum section is used to reduce the wind speed velocity while minimizing losses (Boyle 32). Using a diffuser/plenum before the settling chamber decreases the speed of the air flow for screens and flow straighteners, thus minimizing the power losses because the power losses through the wind tunnel are related to the speed of the fluid cubed (Barlow 91). For this wind tunnel design an equivalent conical expansion angle of six degrees was chosen along with an area ratio of 2:1. This range should prevent boundary layer separation, while decreasing the air velocity. According to Barlow et al. the for most wind tunnel designs the most efficient expansion angle is five degrees – additional savings in expansion angles smaller than this are lost by the additional frictional area losses (Barlow 83). The total loss in the diffuser section is the sum of the frictional losses along its surface area and the expansion losses (Barlow 74). Assuming constant material friction factor the frictional loss can be calculated using Equation 2-1:

Diffuser Frictional Loss Coefficient

$$K_f = \left(1 - \frac{1}{A_R^2}\right) \left(\frac{f}{8 \sin \theta}\right) \quad \text{(Barlow 82)} \quad (2-1)$$

Where:

K_f = Diffuser Frictional Loss Coefficient
 A_R = Diffuser Area Ratio

f = Diffuser Friction Factor
 θ = Diffuser Expansion Angle

The expansion loss equation is experimentally based and depends on the diffuser cross sectional area, and its equivalent conical angle. The expansion loss calculation used is from Eckert et al. The total pressure loss in the diffuser was calculated by adding the frictional loss factor with the expansion loss factor and multiplied by the density and speed squared in Equation 2-2 (Barlow 81-83):

Diffuser Pressure Loss

$$\Delta p_d = (K_f + K_{ex}) \left(\frac{1}{2} \right) (\rho) (V_d)^2 \quad (\text{Barlow 82}) \quad (2-2)$$

Where:

Δp_d = Diffuser pressure loss
 K_f = Diffuser frictional loss coefficient
 K_{ex} = Diffuser expansion loss coefficient

ρ = Fluid density
 V_d = Diffuser fluid entrance velocity

The minimum suggested diffuser/plenum length is approximately the hydraulic diameter of the settling chamber to minimize flow separation and losses (Barlow 81). For diffusers the minimum length is calculated by Equation 2-3:

Diffuser Minimum Length

$$L_d = (R_i) \left[\frac{A_r^{1/2} - 1}{\tan(\theta_d)} \right] \quad (\text{Barlow 81}) \quad (2-3)$$

Where:

L_d = Diffuser Minimum Length
 R_i = Inlet Hydraulic Radius

A_r = Area Ratio
 θ_d = Diffuser Expansion Angle

Settling Chamber

Immediately following the diffuser section is the settling chamber. It is in the settling chamber that the flow velocities are straightened parallel to the center axis and made uniform.

This is a very important section to smooth out irregularities cause by the fan and minor inconsistencies from expansion. In this proposed design there are three turbulence mesh screens and a honeycomb screen. The honeycomb is used to straighten the flow with minimal losses. The mesh screens are used to create a uniform velocity profile, it does this because the flow resistance of the wire is proportional to the speed squared, slowing the faster flow regions more than the slower flow regions. By incorporating a contraction following the settling chamber fewer number of mesh screens are required in the settling chamber to achieve flow uniformity (Bell and Mehta 3). It is suggested by Mehta and Bradshaw that to straighten the flow without impeding it there should be at a minimum approximately 25,000 cells in the honeycomb, which for this wind tunnel correlates to a hydraulic cell diameter of 0.1713 inches (Barlow 91). For the screen pressure loss calculations a screen mesh factor of 1.3 for average circular wire was assumed and used in Equation 2-4 (Barlow 86).

Mesh Screen Loss Coefficient Equation

$$K_m = (K_{mesh})(Re_s)(\sigma_s) + \left(\frac{\sigma_s^2}{\beta_s^2} \right) \quad \text{(Barlow 86)} \quad (2-4)$$

Where:

K_m = Mesh loss coefficient

σ_s = Screen solidity

K_{mesh} = Screen mesh factor = 1.3

β_s = Screen porosity

Re_s = Mesh screen Reynolds Number

Contraction

The contraction component of the wind tunnel increases the incoming fluid velocity while minimizing pressure losses, flow separation, and flow variability. The wind tunnel design uses a two dimensional contraction shape based on Bell and Mehta's fifth-order contraction polynomial. The fifth-order polynomial has been used extensively in many wind tunnels and is a very straightforward design without the need for finite element flow analysis (Bell and Mehta

14). The suggested contraction length range when using the fifth-order polynomial contraction is 0.9 to 1.8; shorter contraction lengths caused exit flow irregularities and long lengths caused boundary layer separation and energy loss (Bell and Mehta 15). Bell and Mehta's fifth order contraction equation used for this project is included as Equation 2-5.

Bell and Mehta's Fifth-Order Contraction Polynomial

$$Y(X) = H_i - (H_i - H_e)[6(X')^5 - 15(X')^4 + 10(X')^3] \quad (\text{Bell and Mehta 15}) \quad (2-5)$$

Where:

H_i = Contraction height at inlet

L = Contraction length

H_e = Contraction height at exit

$X' = X/L$

X, Y, Z = Non dimensional stream wise distance

The two dimension contraction was selected over a three dimensional contraction because it has less boundary layer flow separation and minimizes three dimensional variance (Doolan 1241-1244). According to Bell and Mehta, and substantiated by Doolan, the fifth order polynomial is one of the optimum polynomial of the ones they tested because it has no flow separation at either the centerline nor along the corners, met minimum Reynolds number requirements, and it creates very good flow uniformity (Bell and Mehta 15, Doolan 1244). The pressure loss through the contraction/nozzle was calculated using Equation 2-6:

Contraction/Nozzle Loss Coefficient Equation

$$K_n = (0.32)(f_{av}) \left(\frac{L_n}{D_{ts}} \right) \quad (\text{Barlow 98}) \quad (2-6)$$

Where:

K_n = Nozzle loss coefficient

D_{ts} = Diameter of test section (Nozzle exit diameter)

f_{av} = Average friction factor

L_n = Nozzle length

Test Section

The two main types of test sections are open and closed. For purposes of this wind tunnel design a closed test section will be used because open test sections can have severe flow instability problems and require extensive design flow modeling and corrective measures (Barlow 67). In addition to best model the ABL it is extremely important to manage the turbulence and boundary layer depth, which can be most accurately done in a closed test section. It is suggested that the test section be sized to keep the blockage under 5%, and preferably under 3% (Moonen 702). If the model blocks more than 5% - 10% of the test section, then additional corrections are usually required (Barlow 65). The test section size was limited to minimize the fan size required – the larger the test section the larger and more powerful the fans required to create the same mean wind speed. For the final design turntables will be used in the test section to change the directionality of the prevailing wind on the test models. The loss coefficient through the test section was calculated using Equation 2-7:

Test Section Loss Coefficient Equation

$$K_{ts} = \frac{(f)(L_{ts})}{(2)(R_{ts})} \quad (\text{Barlow 74-75}) \quad (2-7)$$

Where:

K_{ts} = Test section loss coefficient
 f = Friction factor

L_{ts} = Test section length
 R_{ts} = Test section hydraulic radius

The approximate dimensions of the proposed wind tunnel test section are 20' wide by 6' high and 120' long. These overall dimensions were chosen to fit within the building selected to house the wind tunnel. The width was chosen to allowing for large scale low-rise building testing up to the 1:25 scale without exceeding the suggested 5%-10% wind tunnel blockage limit. The height of six feet allows for adequate headroom while setting up experiments within the tunnel.

The length of the wind tunnel was designed to be ten to fifteen test sections heights to allow for adequate boundary layer development.

CHAPTER 3

GOVERNING AERODYNAMIC EQUATIONS

This section describes the overall basic equations upon which most theoretical wind tunnel design calculations are based. There are many books devoted entirely to theoretical and empirical equations for wind tunnels and it would be impractical to describe all of these equations in this report; such references include “Low Speed Wind Tunnel Testing” by Jewel Barlow, et. al. and "Low speed wind tunnel testing” by M.T. Boyle. It is for this reason that the governing aerodynamic equations have been shown in very rudimentary form to explain the general ideas behind the wind tunnel theories and calculations.

As with all Newtonian based problems the principles of conservation of mass and Newton’s Second Law hold true and can be used to help predict fluid flow throughout the wind tunnel. The conservation of mass states that the mass of a closed system will remain constant, regardless of the processes acting inside the system. The continuity equation uses the conservation of mass to establish that from one point in a closed system to another mass is the same, see Equation 3-1.

Continuity Equation

$$\frac{\partial \rho}{\partial t} + \nabla \bullet (\rho \bar{V}) = 0 \quad \text{(Barlow 4)} \quad (3-1)$$

Where:

$\delta \rho$ = Change in fluid density
 δt = Change in time
 ∇ = Divergence

\bullet = Dot Product
 ρ = Fluid density
 \bar{V} = Fluid velocity vector

For low speed applications, defined by Barlow as speed less than 0.3 Mach, the fluid is incompressible and simplifies the continuity equation, See Equations 3-2 and 3-3 (Barlow 13).

The assumption of incompressible flow can be safely assumed because Atmospheric Boundary

Layer (ABL) wind tunnels are almost exclusively run at low wind speeds below mach 0.3 (Barlow 13-14). The simplification of the Continuity Equation with an incompressible flow is shown in Equations 3-4 and 3-5. Using Equation 3-5 the average wind speed can be found in any section of the wind tunnel.

Incompressible Flow Assumption for Low-Speed Applications

$$\frac{\partial \rho}{\partial t} = 0 \quad (\text{Barlow 13}) \quad (3-2)$$

$$\nabla \bullet V = 0 \quad (\text{Barlow 13}) \quad (3-3)$$

Where:

ρ = Fluid density

A = Cross sectional area

\bar{V} = Fluid velocity vector

V = Average velocity of the fluid

Q = Mass Flow

Simplify for Average Two Dimensional Flow Using Eulerian Perspective

$$Q_1 = Q_2 \quad (\text{Auld, Srinivas}) \quad (3-4)$$

$$A_1 V_1 = A_2 V_2 \quad (\text{Auld, Srinivas}) \quad (3-5)$$

Where:

ρ = Fluid density

A = Cross sectional area (See Figure 3-1)

\bar{V} = Fluid velocity vector

V = Average velocity of the fluid g (See Figure 3-1)

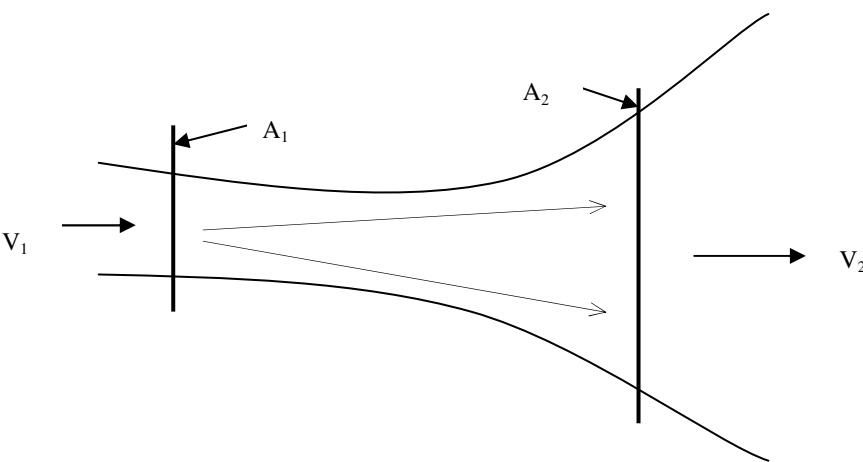


Figure 3-1. Continuity Equation Figure

By applying Newton's Second Law of Motion to an elemental mass with respect to an internal frame of reference with an ideal fluid under steady state conditions in a uniform velocity field the classical Bernoulli Equation is derived. The Bernoulli Equation (Equation 3-6) gives an estimate of the overall velocity pressure relationships throughout the low-speed wind tunnel system; by incorporating frictional and local losses into the Bernoulli Equation (Equation 3-7) it can give estimations of overall system performance and specific pressures can be conducted (Barlow 14):

Bernoulli Equation

$$p_1 + \frac{1}{2}\rho V_1^2 + Z_1 = p_2 + \frac{1}{2}\rho V_2^2 + Z_2 \quad (\text{Auld, Srinivas}) \quad (3-6)$$

Bernoulli Equation with Added Frictional and Local Losses

$$p_1 + \frac{1}{2}\rho V_1^2 + Z_1 - h_f = p_2 + \frac{1}{2}\rho V_2^2 + Z_2 \quad (\text{Auld, Srinivas}) \quad (3-7)$$

Where:

p = Pressure

ρ = Fluid density

V = Average velocity of the fluid

Z = Elevation above datum

h_f = Sum of Frictional and Local Losses

For any fluid flow through a system the loss coefficients for each section can be calculated. These loss coefficients along with the velocity of the fluid in the section, found by using the continuity equation, the known fluid density, and assuming incompressible subsonic conditions (speeds below Mach 0.3), can be used to calculate the average pressure loss across the section, see Equation 3-8. The total pressure loss is calculated by adding up all of the individual section pressure losses (Barlow 74).

Pressure Loss Equation Using a Loss Coefficient

$$\Delta p = (K)\left(\frac{1}{2}\right)(\rho)(V)^2 \quad (\text{Auld, Srinivas}) \quad (3-8)$$

Where:

Δp = Pressure loss

ρ = Fluid density

K = Loss Coefficient

V = Average velocity of the fluid

The circuit energy loss is the energy lost through the circuit through expansion,

contraction, and frictional losses. It is estimated using the total pressure loss in Equation 3-9

(Barlow 73).

Circuit Energy Loss Equation

$$\Delta E_{\text{circuit}} = \frac{(K)\left(\frac{1}{2}\right)(Q)(\rho)(V)^2}{550 \text{ hp}} \quad (\text{Barlow 73}) \quad (3-9)$$

Where:

$\Delta E_{\text{circuit}}$ = Circuit Energy Loss(hp)

V = Average velocity of the fluid (ft/s)

Q = Flow Rate(cfs)

550 hp = horsepower conversion

ρ = Fluid density(slugs/ft³)

Equation 3-9 is only an approximation, as it does not include thermodynamic losses (which should be minimal) or account for the fan efficiency. However, it does serve as a good theoretical minimum bound for error checking because with these losses the test results should always be smaller than this calculated value.

CHAPTER 4

DIMENSIONAL ANALYSIS

Dimensional Analysis of the main fluid mechanics equations of the Navier-Stokes Equation and the Energy Equation lead to four main dimensionless coefficients used to maintain flow similarity – Froude number, Reynolds number, Mach number, and Prandtl number (Barlow 9-15). The Prandtl number is usually neglected in wind tunnels because it mainly deals with the temperature dependent aspect of a fluid, and is usually does not have a significant contribution; see Equation 4-1 (Barlow 11). Mach number is used to represent the proportion of an object of fluid's velocity to that of the speed of sound, See Equation 4-2. In air at 15°C and sea level the speed of sound is 340.3 m/s, 761.2 mph, 1,225 km/h (Clancy 7). To be classified as a “low-speed” wind tunnel it is generally accepted that the Mach number must be below 0.3, making the Mach number also not a significant flow similarity parameter. The Froude number is an important flow similarity for systems where the dynamic interactions between the model and fluid cause unsteady boundary conditions because it takes into account the characteristic wave propagation velocity, see Equation 4-3 (Barlow 10). Since the main purpose of this project is creating an ABL wind tunnel for low-rise structure testing where there will be limited model flexure the Froude number is not usually used for flow similarity. However, to be versatile the wind tunnel will also be able to create stable flows even at very low velocities for Froude number similitude for testing high rise buildings. In general, for applications where the geometry is fixed and the dynamic interactions are neglected such as ABL wind tunnels for testing low rise structures the most significant fluid flow similarity parameter is the Reynolds number (Barlow 11). The Reynolds number is based on the fluid density, viscosity, velocity, and the model's

characteristic length, see Equation 4-4. The Reynolds number maintains the ratio of the inertia force to the viscous force between the full size structure and the model.

Prandtl Number

$$P_r = \frac{\mu C_p}{k} \quad (\text{Barlow 11}) \quad (4-1)$$

Where:

P_r = Prandtl Number

μ = Fluid viscosity

C_p = Specific heat at Constant Pressure

k = Thermal Conductivity

Mach Number

$$M = \frac{v}{v_s} \quad (\text{Clancy 7}) \quad (4-2)$$

Where:

M = Mach Number

v = Velocity of Object or Fluid

v_s = Velocity of Sound in Specified Medium

Froude Number

$$F_r = \sqrt{\frac{V^2}{lg}} \quad (\text{Barlow 10}) \quad (4-3)$$

Where:

F_r = Froude Number

V = Velocity of Object or Fluid

l = Characteristic Length

g = Acceleration of Gravity

Reynolds Number

$$\text{Re} = \frac{\rho V l}{\mu} \quad (\text{Barlow 11}) \quad (4-4)$$

Where:

ρ = Fluid density

μ = Fluid viscosity

V = Velocity of the fluid

l = Characteristic Length

To maintain exact Reynolds number similarity would require very high wind speeds, which can undermine the incompressibility assumption, and/or high performance cooling and pressurized systems to change the fluid properties – all of these solutions require significant capital and maintenance investments. For the purposes of ABL structure modeling where almost all of the models are sharp-edged the effects of Reynolds number are relatively small allowing for a relaxed Reynolds number similarity, saving significantly on the costs of the wind tunnel. For curved bodies critical Reynolds number similarity should be attainable, but only for limited sizes (ASCE 22).

CHAPTER 5

OPEN ABL CALCULATION WORKSHEET

To design the atmospheric boundary layer wind tunnel a Microsoft Excel macro “Open ABL Calculation Worksheet” was created using empirical calculations from various sources. The main source of calculations came from *Low Speed Wind Tunnel Testing* by Barlow, Rae and Pope. This was an excellent source for the sizing and energy loss equations for each section of the wind tunnel. “Performance Requirements and Preliminary Design of a Boundary Layer Wind Tunnel Facility” by Marshall was used for its hydraulic radius equations, and “Contraction Design for Small Low Speed Wind Tunnels” by Bell and Mehta was used for the fifth order polynomial contraction design. The macro Microsoft Excel Solver add-in to perform iterations for the friction factor for each section of the ABL wind tunnel. The Microsoft Excel Solver uses the Generalized Reduced Gradient (GRG2) nonlinear optimization code that was developed by Leon Lasdon, University of Texas at Austin, and Allan Waren, Cleveland State University (Microsoft).

The Open ABL Calculation Worksheet uses a series of givens to design an atmospheric boundary layer wind tunnel. The “Givens” page of the worksheet allows the user one simple place to enter in all their constraints, See Figure 5-1. The “Givens” page has suggestions based on the literature research to assist the user in defining the constraints. As a check conditional formatting has been added to notify the user if their selected constraint falls outside the suggested range. This is achieved by changing the cell background color from green to yellow or red, depending on how far the value is from the suggested range. The macro will still run outside of the suggested ranges, but just notifies the user. After the user is done entering the information

they simply click the “Calculate” button and the macro takes over calculating all the suggested lengths, pressure drops, and energy losses.

Given	Value	Given	Value
Maximum Prototype Height (ft)	1.5	Safety/Wire Screen Diameter: d_w (in)	0.125
Maximum Prototype Length (ft)	4	Safety/Wire Screen Cell Width: W_m (in)	2.50
Model Scale	1/10	Safety/Wire Screen Mesh Factor: K_{mesh} (Suggested 1.3)	1.30
Maximum Fan Flow Q (cfm)	7,650	Mesh Screen Mesh Factor: K_{mesh} (Suggested 1.3)	1.30
Blockage Allowed (Max 10%, Safe 5%)	5%	Mesh Screen #1 Wire Diameter: d_w (in)	0.00748
Test Section Height: H_{ts} (Min 6 ft)	0.6	Mesh Screen #1 Cell Width: W_m (in)	0.50000
Test Section Width: W_{ts} (Suggested: 10ft - 20ft)	2	Mesh Screen #2 Wire Diameter: d_w (in)	0.00748
Test Section Development: L_{ts} (ft)	10	Mesh Screen #2 Cell Width: W_m (in)	0.37500
Maximum Circular Model Diameter (Suggested: 0.5ft)	0.5	Mesh Screen #3 Wire Diameter: d_w (in)	0.00748
Inlet Height: H_i (ft)	3	Mesh Screen #3 Cell Width: W_m (in)	0.26087
Inlet Width: W_i (ft)	3	Honeycomb Cell Hydraulic Diameter: D_h (in)	0.152
Diffuser Length: L_d	3.00	Honeycomb Length to Cell Diameter Ratio: L_h/D_h	13.12
Diffuser Area Ratio: A_R (Suggested 2:1 to 4:1)	1.00	Honeycomb Porosity: β_h (Suggested 0.8)	0.80
Plenum Area Ratio: A_R (1:1)			

Calculate

Figure 5-1. Open ABL Calculation Worksheet: “Givens” Page

After clicking the “Calculate” Button the user is taken to the “Calculations” page and shown all the constants, references, conversions, and equations with their results for each section of the wind tunnel. Figure 5-2 shows the first of five pages of output.

Constants	References
$\nu = 1.70E-04$ ft ² /s	1. Barlow, Jewel B., William H. Rae, and Alan Pope. <u>Low Speed Wind Tunnel Testing</u> . 3rd ed. New York: Wiley-InterScience, 1999.
$\mu = 3.7373E-07$ lb-s/ft ²	2. Marshall, Richard D., 1985, “Performance Requirements and Preliminary Design of a Boundary Layer Wind Tunnel Facility,” National Bureau of Standards U.S. Department of Commerce Rep. No. NBSIR 85-3168.
$\rho = 0.002378$ slug/ft ³	3. Bell, J. H., and Mehta, R. D., 1988, “Contraction Design for Small Low Speed Wind Tunnels,” NASA Contractor Rep. No. NASA-CR-177488.
1 mph = 1.466666667 fps	
1 hp = 550 ft-lb/s	
1 ft = 12 in	
1 cfm = 0.016666667 cfs	

Given Conversions	Value	Equations
Flow Rate: Q (cfs)	128	1 cfm = 0.016666666667 cfs
Maximum Prototype Area (ft ²)	6	Prototype Area = (Prototype Height)(Prototype Length)
Maximum Model Area (ft ²)	0.06	Maximum Model Size = (Maximum Model Area)(Model Scale) ²
Maximum Wind Velocity: V_t (mph)	72.4	1 mph = 1.4666666666666666 fps
Test Section Area: A_{ts} (ft ²)	1.2	Section Area = (Section Height)(Section Width)
Inlet Section Area: A_i (ft ²)	9	Inlet Area = (Inlet Height)(Inlet Width)
Safety Screen Wire Diameter: d_w (ft)	0.010417	1 ft = 12 in
Safety Screen Cell Width: W_m (ft)	0.208333	1 ft = 12 in
Mesh Screen #1 Wire Diameter: d_w (ft)	0.000623	1 ft = 12 in
Mesh Screen #1 Cell Width: W_m (ft)	0.041667	1 ft = 12 in
Mesh Screen #2 Wire Diameter: d_w (ft)	0.000623	1 ft = 12 in
Mesh Screen #2 Cell Width: W_m (ft)	0.031250	1 ft = 12 in
Mesh Screen #3 Wire Diameter: d_w (ft)	0.000623	1 ft = 12 in
Mesh Screen #3 Cell Width: W_m (ft)	0.021739	1 ft = 12 in
Honeycomb Cell Hydraulic Diameter: D_h (ft)	0.012700	1 ft = 12 in

Wind Tunnel Specifications	Value	Equations	Ref
Minimum Test Area (ft ²)	1.2	Minimum Test Area = (Maximum Model Size)/(Blockage Allowed)	1
Maximum Wind Velocity: V_t (fps)	106	$V_t = (Q)/(A_{ts})$	1
Critical Reynolds Number: Re_{cr}	3.13E+05	$Re = (V_t)(Circular Diameter)/(v)$	2
Jet Power: P_t (hp)	3.11	$P_t = (0.5)(\rho_t)(A_i)(V_t)^2/(550hp)$	1
Initial Pressure Drop: Δp_i (psf)	13.423	$\Delta p_i = (1/2)(\rho)(V_d)^2$	1

Figure 5-2. Open ABL Calculation Worksheet: “Calculations” Page 1 of 5

The macro compiles the solutions for each of the sections and then creates a series of graphs to visually demonstrate the pressure distribution, the wind tunnel vertical cross section and plan view, See Figure 5-4 and Figure 5-4.

Atmospheric Boundary Layer Windtunnel

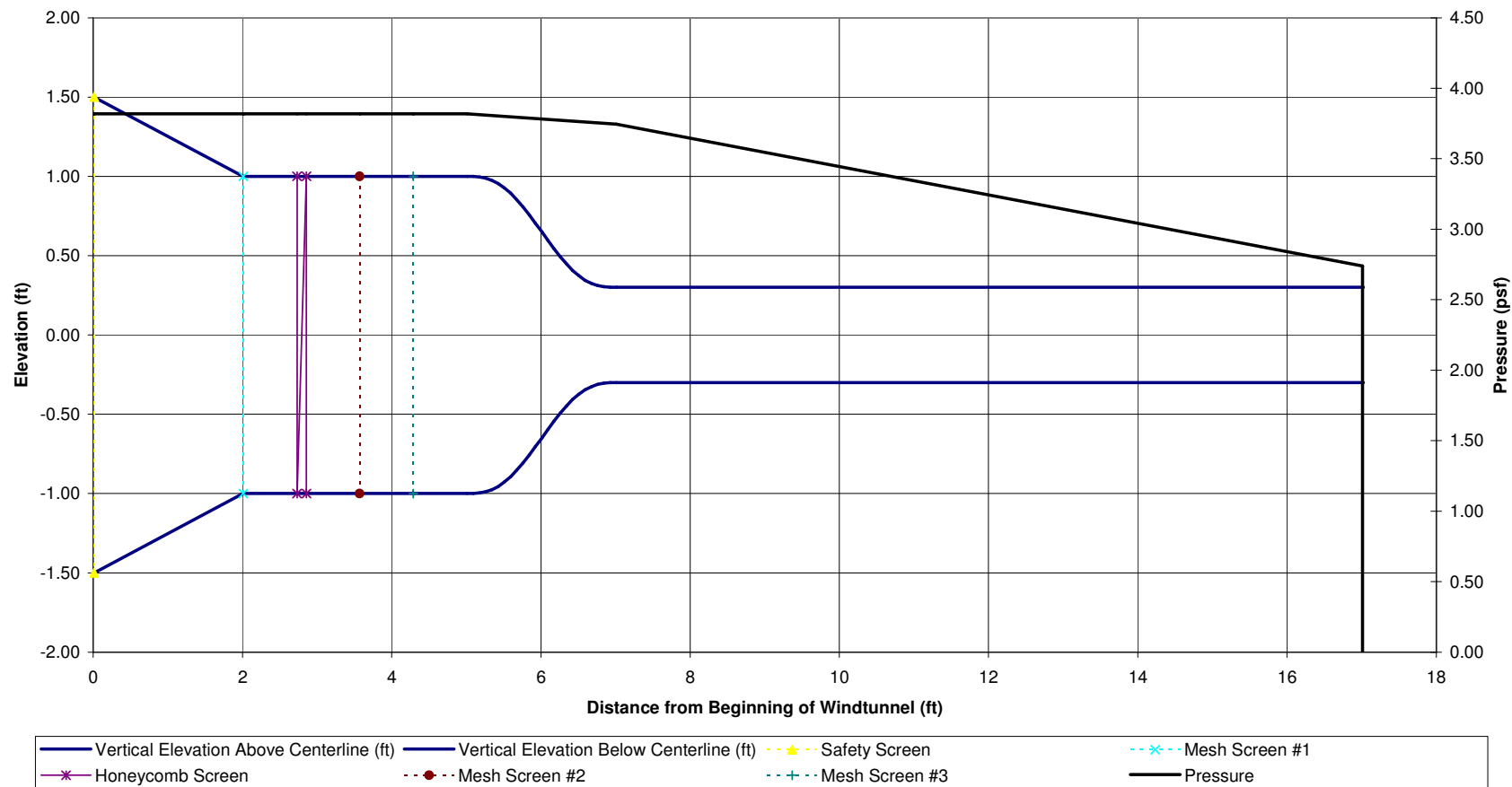


Figure 5-3. Open ABL Calculation Worksheet: Vertical Cross Section with Pressure Distribution

Atmospheric Boundary Layer Windtunnel Plan View

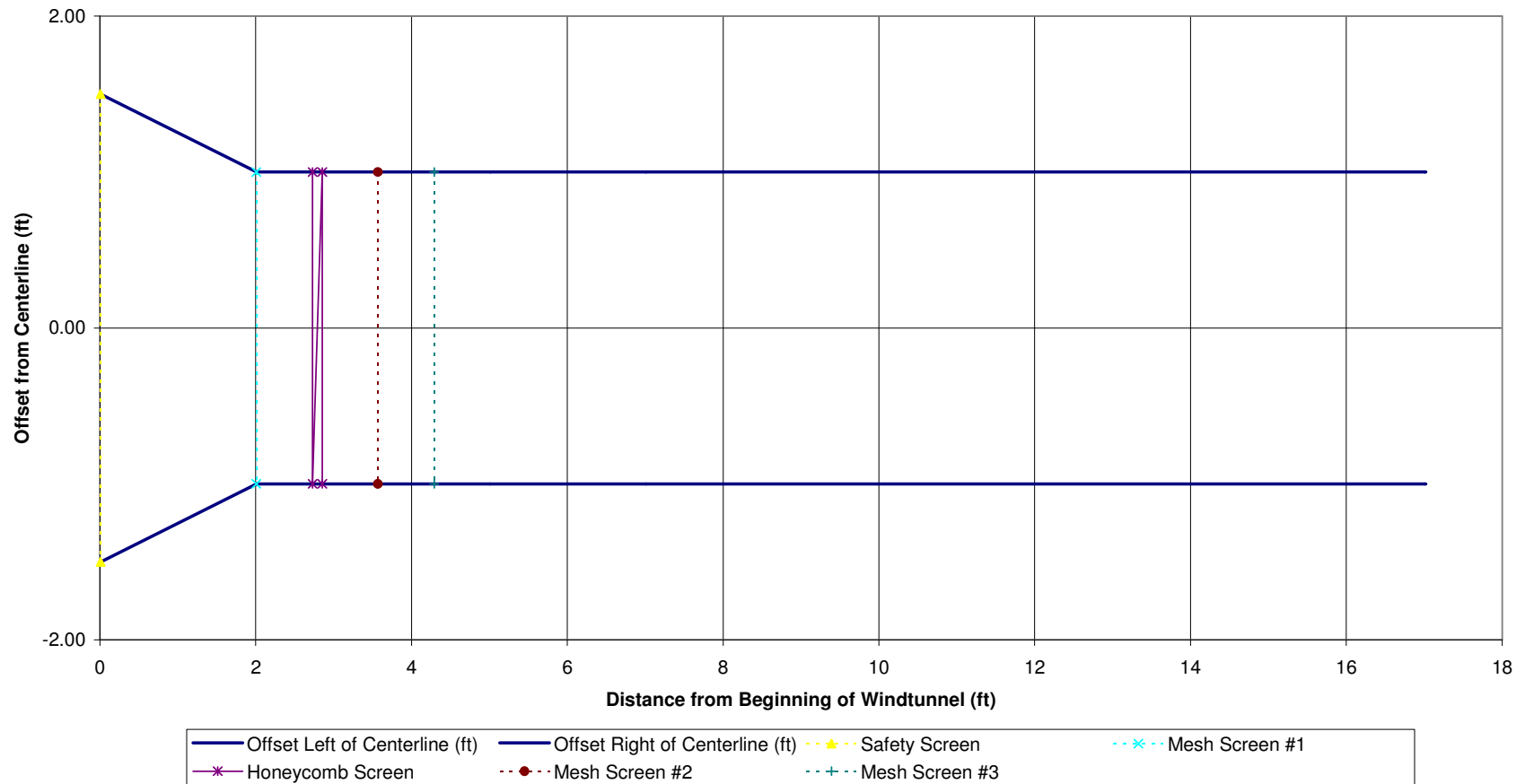


Figure 5-4. Open ABL Calculation Worksheet: Plan View

The Open ABL Calculation Worksheet is limited to open return Low Speed Atmospheric Boundary Layer Wind tunnels with the layout in this order: Fan, Diffuser/Plenum, Settling Chamber, Contraction, and Test Section. It is also limited to a two-dimensional contraction scheme using Bell and Mehta's fifth order polynomial (Doolan 1242). This worksheet is based on empirical equations, and should only be used for preliminary design because it does not have the accuracy or complexity of a finite element analysis.

The worksheet's limitations aside, using this macro as a base it can be easily modified to use other layouts and contraction equations by modifying the equations in the calculation page. As discussed later in this paper the results from the Open ABL Calculation Worksheet correlate very closely with testing performed on the ABL model wind tunnel created for this project. This makes this Open ABL Calculation Worksheet a very versatile instrument for Atmospheric Boundary Layer preliminary design and education. The complete worksheet with all the equations and calculations used for this wind tunnel is included as Object 5-1. Open ABL Calculation Worksheet (.xls file 155KB).

[Object 5-1. Open ABL Calculation Worksheet \(.xls file 155KB\)](#)

CHAPTER 6 CONSTRUCTION

Axial Fans

The total pressure gradient that must be produced by the fan was calculated by summing the individual component pressure losses of each section throughout the entire system. The minimum flow from the fans required to achieve the required test section velocity was calculated using the following equation based on the Continuity of Mass:

Minimum Fan Flow Required

$$\text{Flow Rate} = (V_f)(A_t)$$

Where:

$$V_f = \text{Maximum test section wind velocity} \qquad A_t = \text{Test section cross sectional area}$$

The fan selected for this project is a 26 inch fan manufactured by Patterson Fan Company, Inc, see Figure 6-1. The propeller is 26 inches in diameter and consists of three blades of galvanized aluminum each angled at 18 degrees (Patterson Fan Inc.). For the preliminary testing the propeller operates at a standard 1800 rpm (Patterson Fan Inc.). The fan can be manufactured to use a variety of voltages ranging from 115V, 220V, or 277V (Patterson Fan Inc.). Since this is a model wind tunnel versatility is very important. The 115V was selected because it is more readily available in the United States so that the wind tunnel can be setup in a variety of different buildings for demonstrations. The 115V model uses 13.4 motor amps and 12.4 running amps of power to run the 1 horsepower motor (Patterson Fan Inc.). The maximum flow is estimated at 7650 cfm creating velocities in excess of 575 feet per second without any backpressure, exceeding the minimum flow requirements of the model wind tunnel; an estimated flow pattern is show in Figure 6-2 (Patterson Fan Inc.). For this preliminary design the fan was not equipped with a speed regulator, but could be for future testing to regulate the wind speed in the test

section. The fan was permanently mounted on a stand which was attached to the table by bolts to ensure a very sturdy base to minimize vibrations. A total of three tables were used, the fans and settling chamber on one table and the test section on the two other tables. By using separate tables vibrations from the fan were not transferred to the test section and instrumentation.

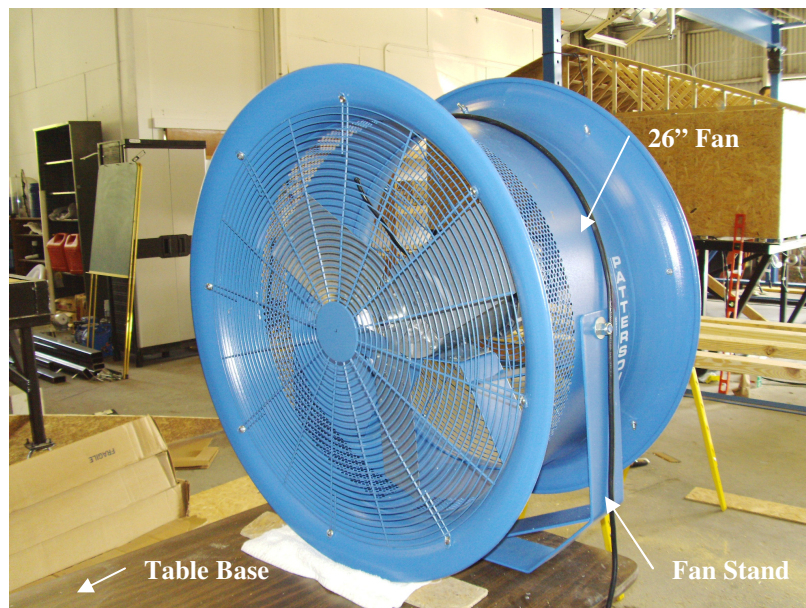


Figure 6-1. 26 inch High Velocity Patterson Fan

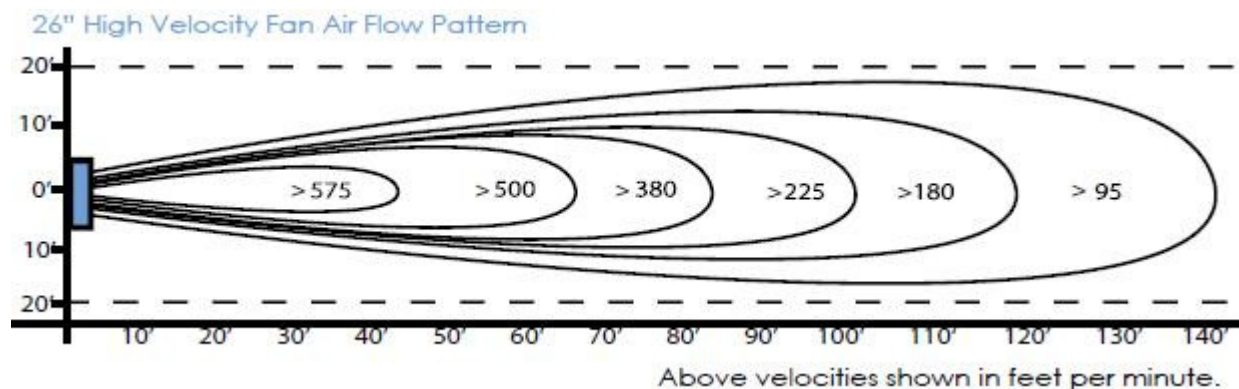


Figure 6-2. 26 inch High Velocity Fan Air Flow Pattern

Diffuser/Plenum

For this project the minimum size fan that would produce adequate flow was 26 inch diameter, and the settling chamber was selected to be 24 inches by 24 inches square, so a plenum

was used to change the circle to a square. Since a plenum was used there was no expansion loss coefficient, but there still was frictional losses. The plenum was constructed of 3mm Sintra PVC 24" x 36" sheets because it is easily bendable, durable, and resilient enough to withstand the wind tunnel forces. A template from two pieces of plywood was created with the fan diameter on one side and the settling chamber 2'x2' square on the other. It was then attached with 2x4's so that the centers aligned. Eight holes were drilled around each shape and clothes hangers were strung to create the three dimensional plenum, See Figure 6-3. A heat gun was used to then form the Sintra boards around the clothes hangers, creating a smooth and constant plenum shape. The plenum was then attached to the settling chamber using liquid nails adhesive and rivets, See Figure 6-4. Rivets were used because unlike screws or bolts they do not protrude into the wind tunnel causing flow irregularities. After initial construction all of the corners were sealed with silicone caulking to minimize exfiltration and all the overlaps were taped with foil tape. Foil tape was used in place of duct tape because of its very smooth surface minimizing losses and flow irregularities, as well as its increased longevity. The plenum was finally attached to the fan using a combination of foil tape to minimize losses and duct tape for structural strength.

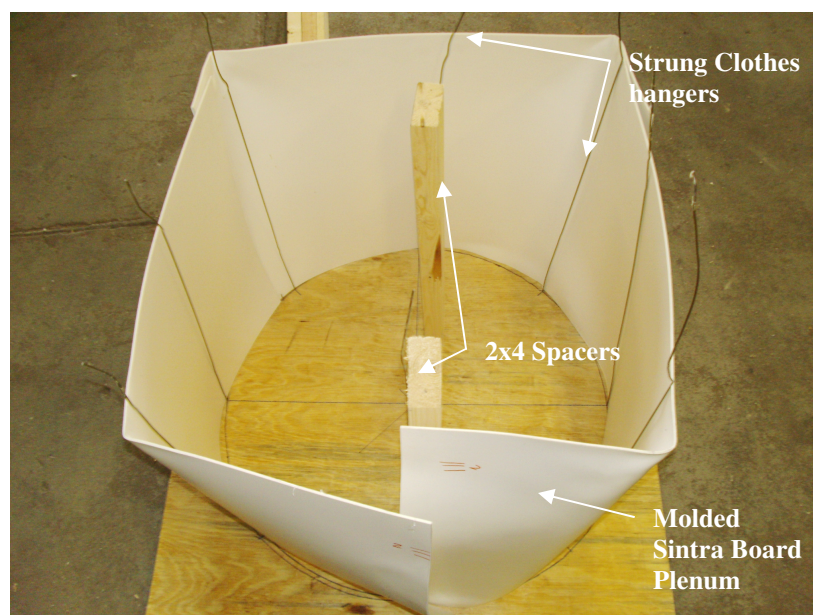


Figure 6-3. Plenum Construction Template

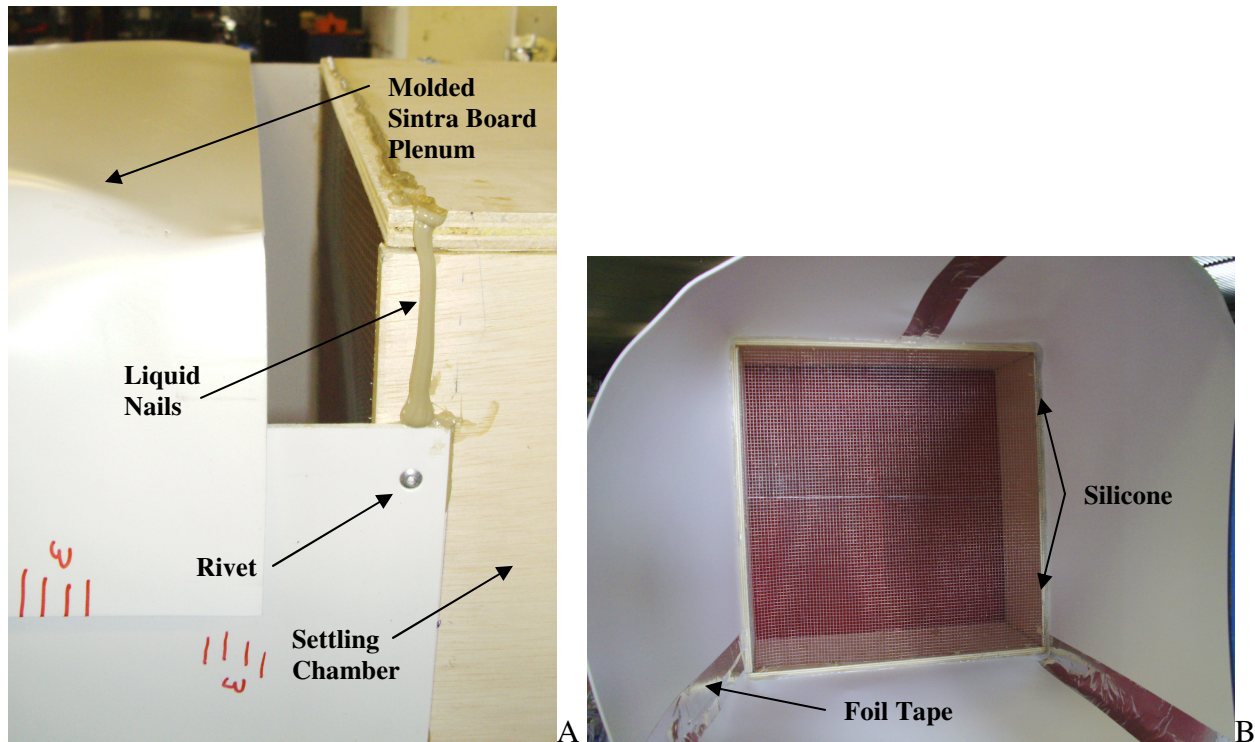


Figure 6-4. Plenum Construction: A) Attachment with Rivets and Liquid Nails B) Weather stripping with Silicone Caulking and Foil Tape

Settling Chamber

Price quotes from three metal manufacturing companies placed the total cost for a fabricated honeycomb between \$1,000 and \$1,400 plus taxes and shipping and handling. Because of budget constraints the honeycomb was created by hand using thin red drinking straws, which were 0.1524 inches in diameter, meeting the minimum requirements set by Mehta and Bradshaw. The straws were held in place with a gallon of Elmer's glue because of its low cost, long setting time, non-reactivity with the straws, easy cleanup, and ease of application. First a settling chamber was created from 2'x3' finished pieces of $\frac{3}{4}$ " sandply attached together with metal angles. A piece of cardboard was cut to the shape of the settling chamber to create a uniform flat surface to place the drinking straws against. The cardboard was covered with wax paper to minimize the sticking and placed perpendicular to the walls. Next thousands of 8 inch

long thin drinking straws were cut into 1.5 inch lengths using a cutting template. Each of the 35,000+ straws was then hand placed one at a time in a row with two rows of glue on top. The honeycomb was reinforced by placing 3/4" inch 1/16 inch thick Aluminum rod midpoint to midpoint across the chamber vertically and horizontally. The total material cost for hand constructing the honeycomb out of straws and glue was approximately \$75 (See Table 6-1) for an estimated savings of over \$1,000.

After the honeycomb construction was finished the mesh was installed. For this design wire diameters of 19 gauge (0.0359 inches diameter) with cell widths of 1/2" inch to give a uniform flow with minimal loss. This wire cell widths and diameter were well within the suggested mesh required according to Doolan. In his paper Doolan increased mesh densities until flow the exit plan uniformity was at an acceptable level. It was found that the 150x20x20 cells in the X, Y and Z directions mesh was sufficient to accomplish that acceptable level in his investigation (Doolan 1242).

The mesh was cut to be approximately 1 inch oversized so that the edges could be stapled to the inside of the settling chamber. One mesh was placed before the honeycomb and two were placed after the honeycomb. A picture of the completed settling chamber with the mesh screens and honeycomb can be seen in Figure 6-5. The exact locations of the mesh and honeycomb within the settling chamber can be seen in Figure 5-4.

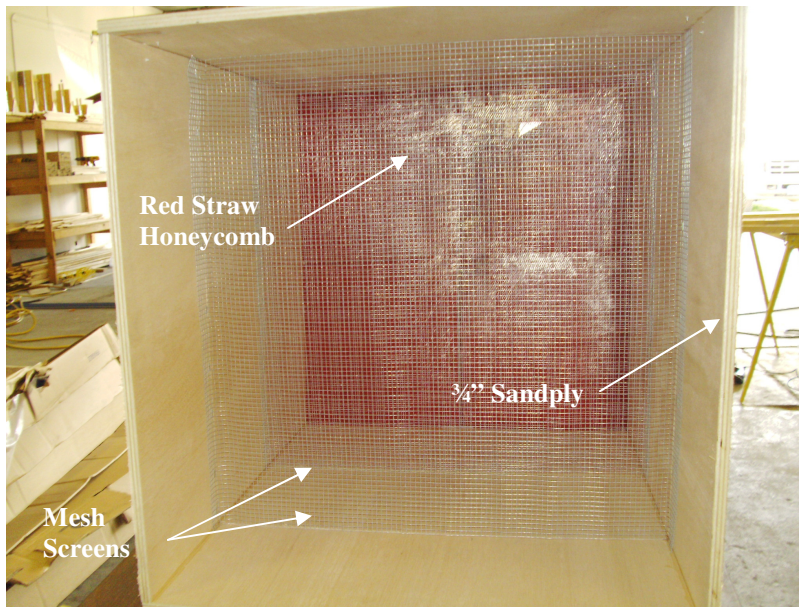


Figure 6-5. Completed Settling Chamber with Honeycomb and Mesh Screens

Contraction

The contraction for the model wind tunnel was constructed by first creating a template. For this project the length of the nozzle is equal to the height of the settling chamber to minimize the flow non-uniformity without boundary layer separation or too much energy loss. The Bell and Mehta fifth order polynomial was plotted in Microsoft Excel and printed to scale. The printout was then attached to plywood and used as a guide for the clothes hanger holes. 2x4's were attached and clothes hangers were strung between the two boards, See Figure 6-6. The Sintra boards were then molded to the form using a heat gun creating the top and bottom sections of the contraction. The sides were created by attaching the paper template to two Sintra boards and cutting the pattern using a jigsaw, See Figure 6-7A. All the contraction pieces were attached to both the settling chamber and the test section using a combination of rivets, liquid nails, foil tape and duct tape, See Figure 6-7B. The top of the test section was attached to the contraction using only foil tape so that the top section can be removed in the future for research.

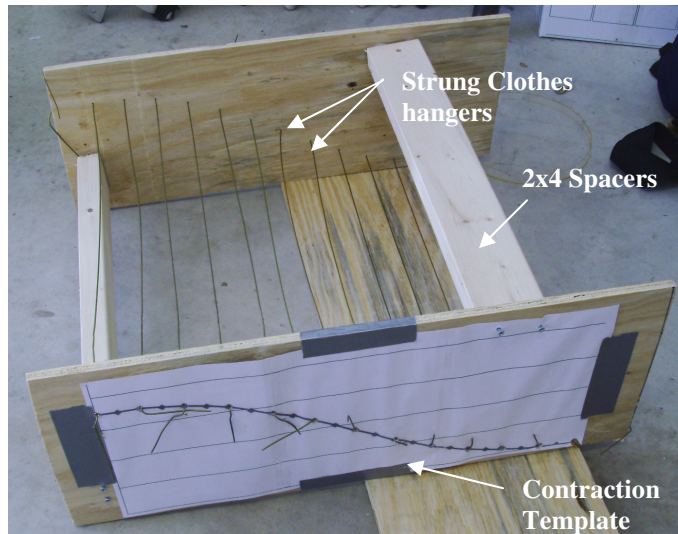


Figure 6-6. Contraction Template

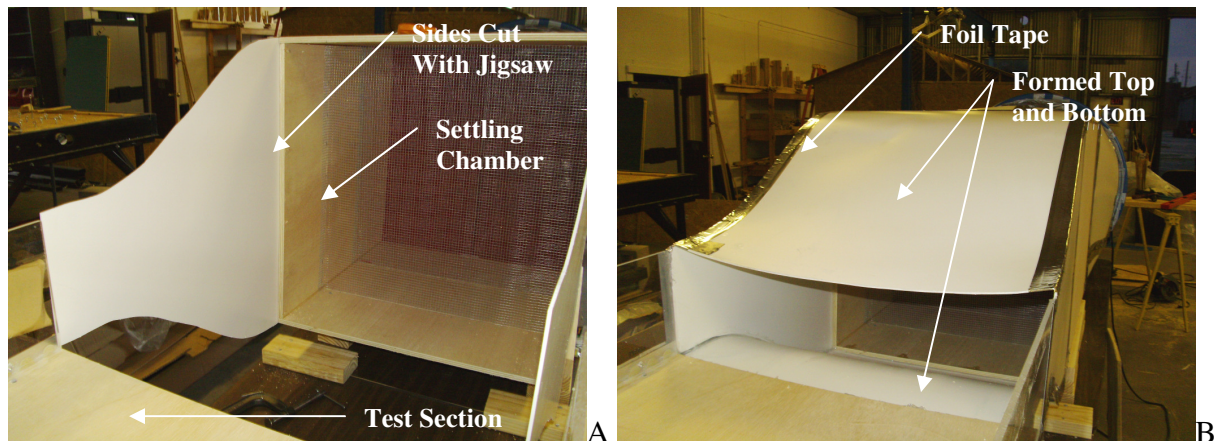


Figure 6-7. Contraction Construction: A) Side Construction B) Completed Construction

Test Section

The test section side walls for the model wind tunnel were constructed from 1/4" thick cast transparent Plexi-glass to allow for easy model and flow viewing; this is especially important if smoke is used for streamlines viewing. The test section top and bottom sections was constructed from 3/4" sandply to minimize costs. The bottom and sides of the wind tunnel were attached by riveting 1 In. x 1/16 in. thick Aluminum angle to each of the pieces. Liquid nails was also used for additional structural rigidity. All of the inside corners and joints were then sealed with

silicone caulk to minimize roughness and flow instability. The top piece had the Aluminum angle and weather stripping attached to its edges. The top of the test section was temporarily attached using yellow tie downs to the bottom and sides to allow for its future removal for additional research in boundary layer creation. The bottom section can be seen being caulked in the foreground of Figure 6-8A, with the top section laying upside down with the angles attached in the background. Supports were created to raise the test section vertically along the wind tunnel's centerline. The supports were created from 4x4's set vertically and reinforced horizontally by 2x4's as shown in Figure 6-8B. 2x4's were run parallel to the test section bottom between the 4x4's to create stable base. The supports were glued and screwed to the table using 4" decking screws for increased stability and rigidity

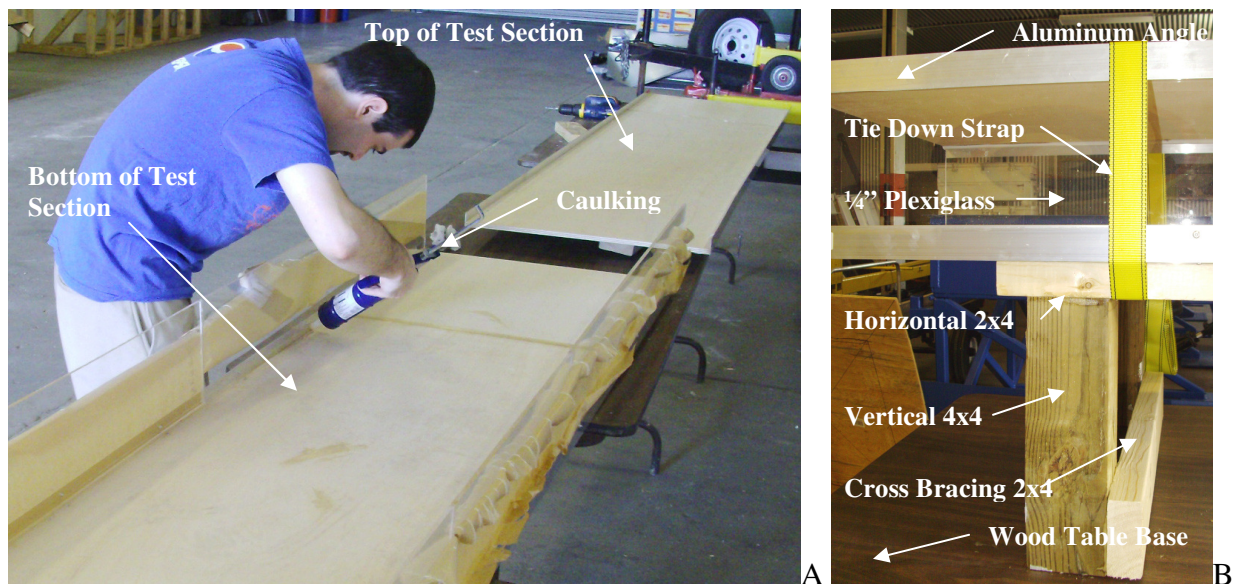


Figure 6-8. Test Section Construction: A) Caulking Interior Corners B) Reinforced Support and Tie Down

Completed Wind Tunnel

The total construction of the wind tunnel took over a year from January 2008 when the project literature review started to April 2009 when the paper was completed. Most of this time was spent constructing the honeycomb. Construction of the honeycomb took 12 hours a day for

three months. The first month consisted of cutting the 35,000+ straws to length and preparing the settling chamber walls. The next two months was installing the 35,000+ straws in the wind tunnel housing. It took such a long time to install because before installation two beads of glue had to be placed and each straw had to be inspected to make sure both ends were not cold fused together from the cutting. Placement add to the time because of the need to minimize the infiltration of the glue into the straw openings and to properly align all of the straws parallel to the centerline. It took one 12 hour days to cut and install all the pieces of the test section, and one 12 hour days to create the templates and mold the sections for the plenum and contraction. By constructing each section ahead of time final assembly took only one 12 hour day, which consisted mostly of building the proper supports and leveling and centering each of the sections. Figure 6-9 shows the completed ABL wind tunnel with each of its sections.

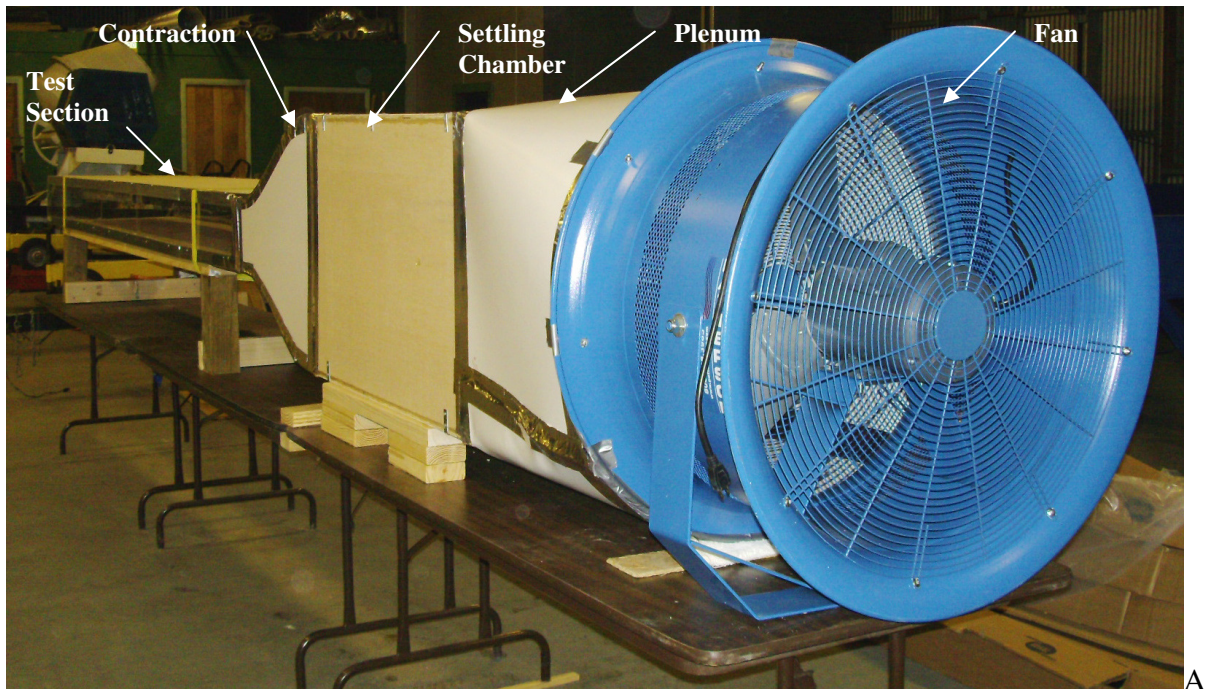




Figure 6-9. Completed Wind Tunnel

The final total cost for the wind tunnel construction came to \$1,855.71 under budget. This number slightly underestimates the total cost of the ABL wind tunnel construction because there were some additional items such as duct tape and screws that we used and that are not easily accountable. A complete breakdown of the major components of the ABL wind tunnel is included as Table 6-1.

Purpose Material (unit)	Cost Per Unit	Number of Units	Shipping and/or Taxes	Subtotal	Suppliers
Fan					
26 Inch High Velocity Fan (each)	\$790.00	1	\$166.50	\$956.50	http://www.pattersonfan.com/
Settling Chamber					
Test Section Top/Bottom					
3/4" x 4' x 8' Sandply (each)	\$45.87	2	\$5.73	\$97.47	Home Depot
Honeycomb Section					
8" Red Drinking Straws (5,000 ct)	\$30.21	2	\$0.00	\$60.42	http://www.instawares.com/
Mesh Section					
19 guage 1/2" mesh fence (36"x10')	\$14.47	2	\$1.81	\$30.75	Lowes
Test Section Side Panels					
9" x 48" - Clear Acrylic Plexiglass Sheet - 1/4" Thick Cast (each)	\$14.80	5	\$14.58	\$88.58	http://www.estreetplastics.com/
Plexiglass Cutter (each)	\$5.00	1	\$0.31	\$5.31	Home Depot
Contraction/Plenum Sections					
3mm Sintra PVC 24" x 36" x 3mm (10 sheets)	\$167.40	1	\$21.81	\$189.21	http://foamboardsource.com/
Milwaukee 1220 Heat Gun (each)	\$19.99	1	\$1.25	\$21.24	Home Depot
Reinforcing					
1 In. x 10 ft., 1/16 In. Thick Angle, Aluminum (each)	\$20.94	4	\$5.24	\$89.00	Home Depot
3/4" In. x 8 ft., 1/16 In. Thick Rod, Aluminum (each)	\$19.57	1	\$1.22	\$20.79	Home Depot
1.5" Angle Brackets (4 pack)	\$7.85	2	\$0.98	\$16.68	Home Depot
Adhesive					
Liquid Nails Project (each tube)	\$1.57	5	\$0.49	\$8.34	Home Depot
Rivet Tool (each)	\$19.91	1	\$1.24	\$21.15	Home Depot
Rivets Long (50 pack)	\$4.96	2	\$0.62	\$10.54	Home Depot
Rivets Medium (50 pack)	\$5.19	2	\$0.65	\$11.03	Home Depot
Elmer's Glue (gallon)	\$15.59	1	\$0.97	\$16.56	Office Depot
Caulk Gun (each)	\$9.99	1	\$0.62	\$10.61	Home Depot
Weatherstripping					
Silicone Caulk (each tube)	\$4.97	4	\$1.24	\$21.12	Home Depot
Weatherstripping (17' Length)	\$9.89	2	\$1.24	\$21.02	Home Depot
Base					
6' Wood Table	\$50.00	3	\$9.38	\$159.38	Office Depot
Grand Total				\$1,855.71	

Table 6-1. ABL Wind Tunnel Materials, Costs, and Suppliers

CHAPTER 7

MODEL WIND TUNNEL TESTING

Testing Setup

The wind tunnel testing was conducted using the following materials: Series 100 Cobra Probe by Turbulent Flow Instrumentation, a TFI Interface Unit with cords, a laptop computer with internet access, a traverse, two screw clamps, a wood base, 3 feet of reference port tubing, tape measure, drill, and infrared thermometer, See Figure 7-1.

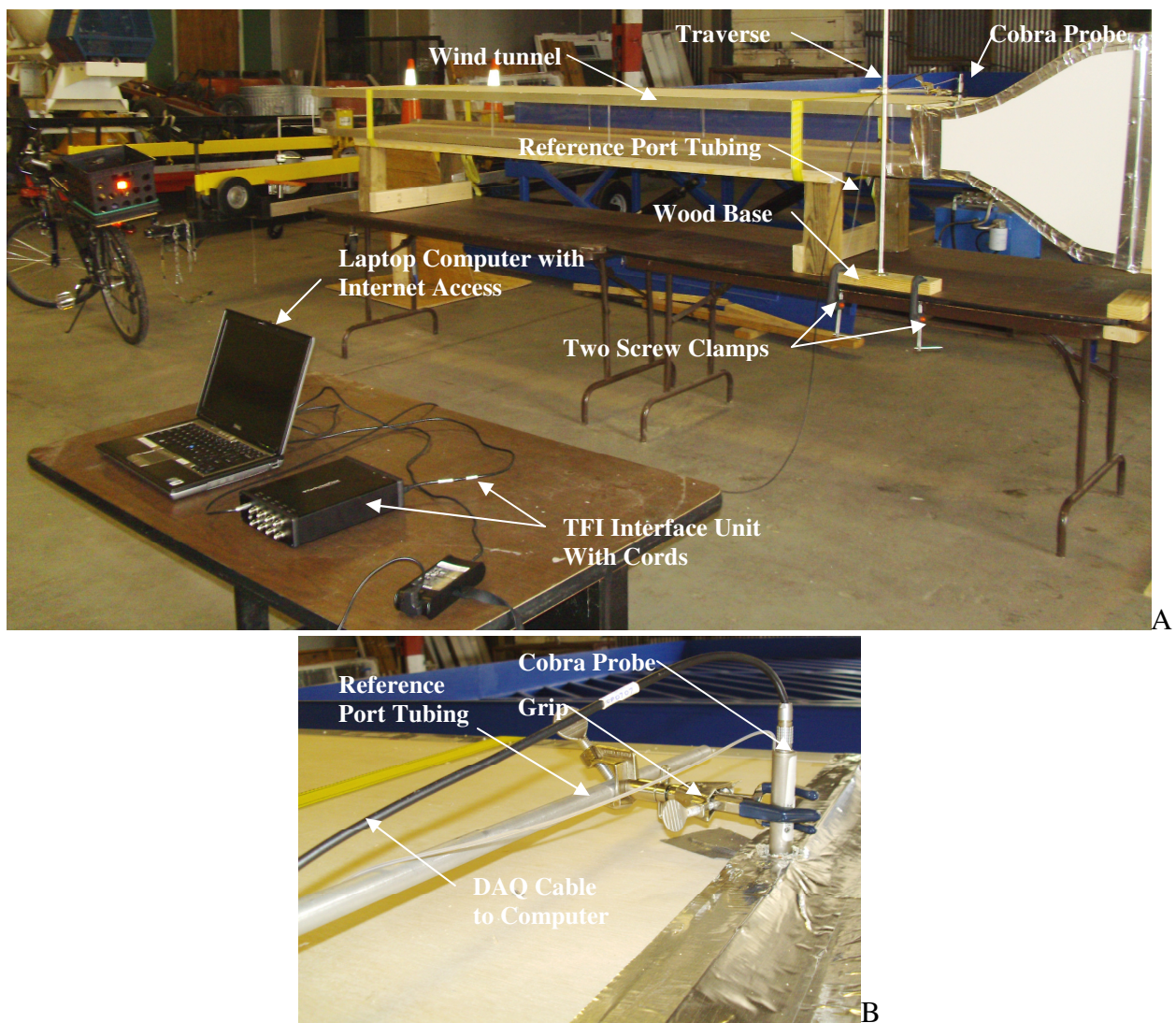


Figure 7-1. Cobra Probe Testing Setup: A) Computer B) Setup Probe Close-Up

Cobra Probe and TFI Data Acquisition Software

The following is a description of the Series 100 Cobra Probe from the manufacturer

Turbulent Flow Instrumentation:

The Cobra Probe is a multi-hole pressure probe that provides dynamic, 3-component velocity and local static pressure measurements in real-time. The Probe is capable of a linear frequency-response from 0 Hz to more than 2 kHz and is available in various ranges for use between 2 m/s and 100 m/s. It can measure flow angles in a $\pm 45^\circ$ cone, all six Reynolds stresses and allows calculation of other higher order terms. Probes are supplied fully calibrated and ready to use.

The Cobra Probe consists of a connector, main body, reference pressure port, stem, and head, See Figure 7-2 (Turbulent Flow Instrumentation). For this testing the manufacture supplied small plastic tube was placed over the reference pressure port and run away from the wind tunnel to ensure an outside reference pressure that was unaffected by the wind tunnel.

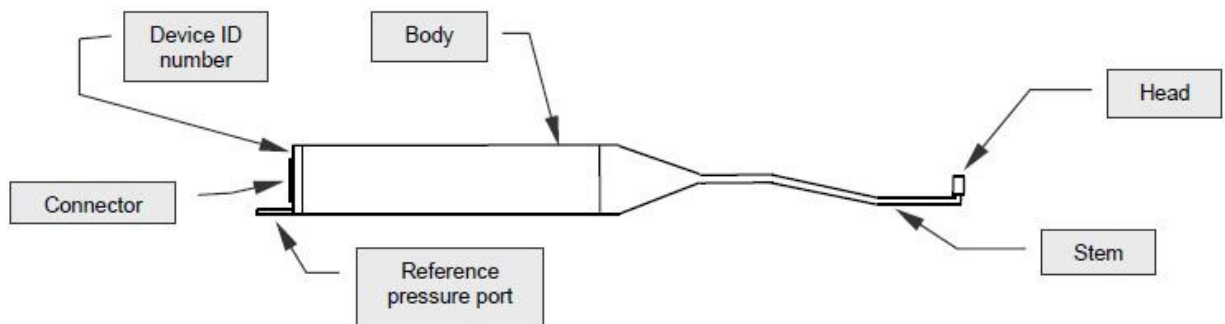


Figure 7-2. Cobra Probe Layout

The Cobra Probe is a very versatile instrument that is capable of simultaneously recording many different flow attributes: Mean Reference Pressure, Mean Flow Speed, Pitch Angle, Yaw Angle, Static Pressure, U, V, W, Minimum and Maximum Velocities, Turbulence Intensities,

Reynolds Normal Stress, and Reynolds Shear Stress. The readings are based on the axis system noted in Figure 7-3 (Turbulent Flow Instrumentation). In the test section the X-direction is the longitudinal component, the Y-direction is the transverse component, and the Z-direction is the vertical component.

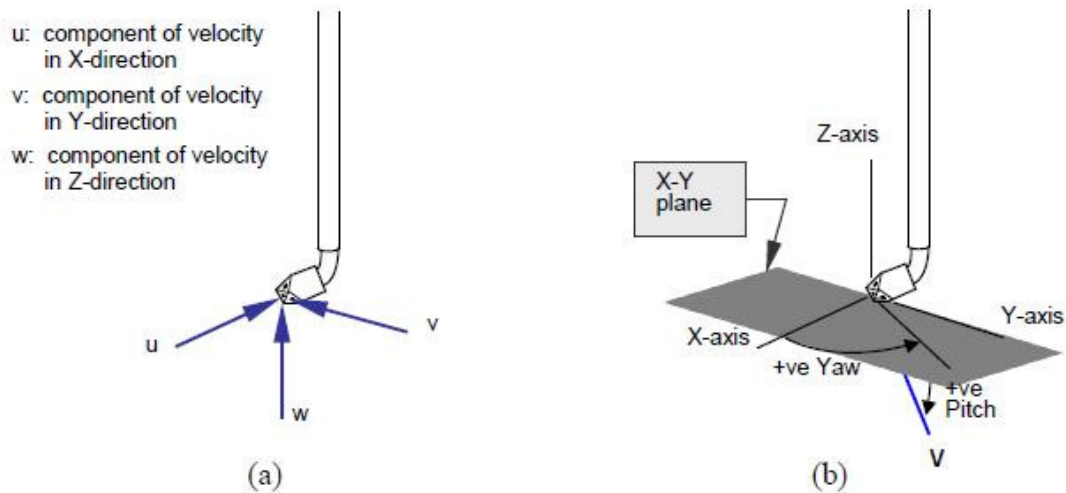


Figure 7-3. Cobra Probe Axis System

The Cobra Probe Manufacturer also included their own data acquisition software that was used for this testing called “TFI Device Control,” See Figure

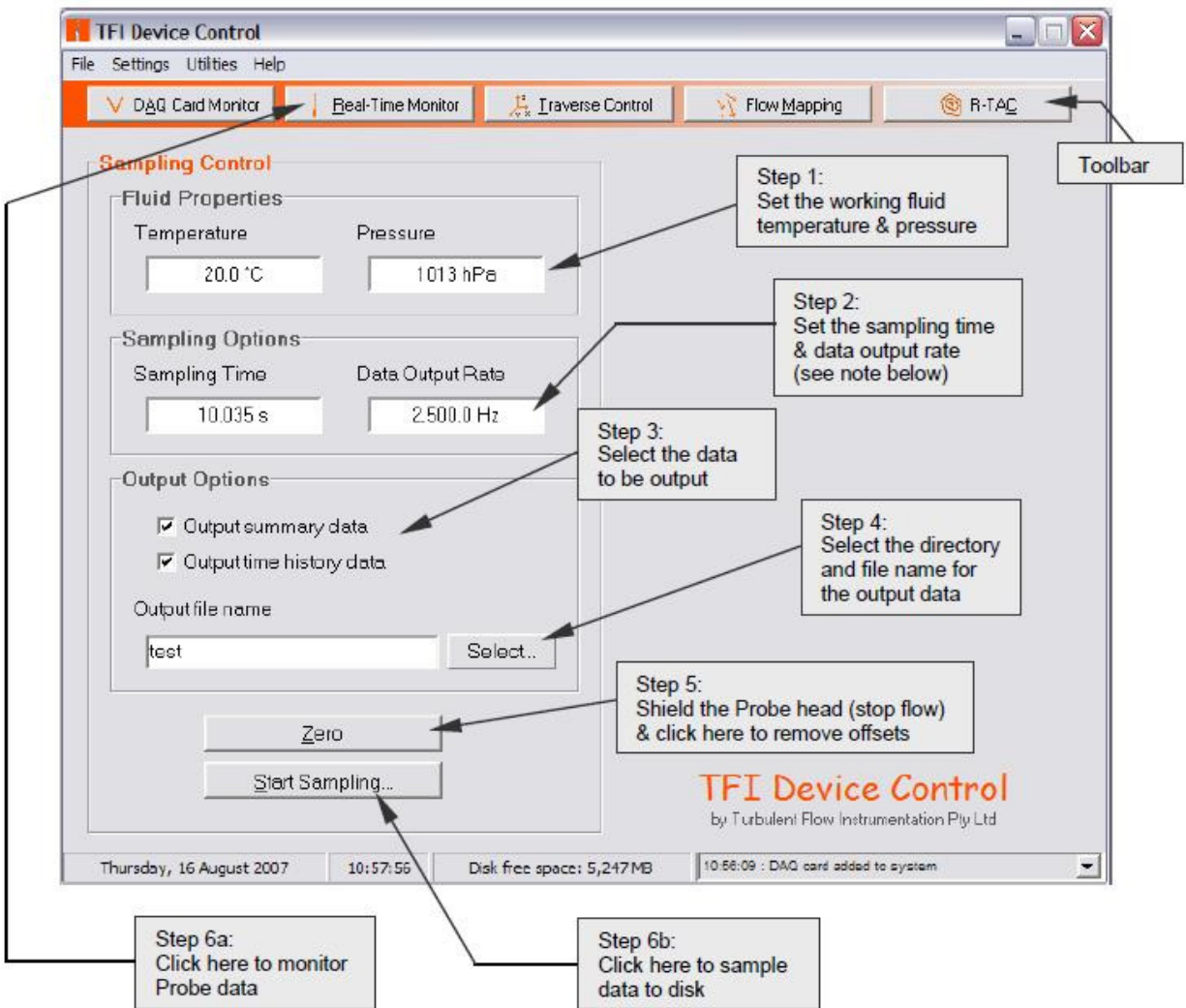


Figure 7-4 (Turbulent Flow Instrumentation).

For the ABL wind tunnel testing fluid properties the temperature was based on an infrared thermometer pointed at the wind tunnel, and the barometric pressure was found online from the Gainesville Airport weather station, located a few blocks from the testing site. The temperature ranged from 23.9°C to 26.4°C, and the barometric pressure remained constant at 102,167.9 Pa throughout the testing. The sampling options were set with the sampling time at 120 seconds sampling at 5,000 hertz and outputting at 2,500 hertz.

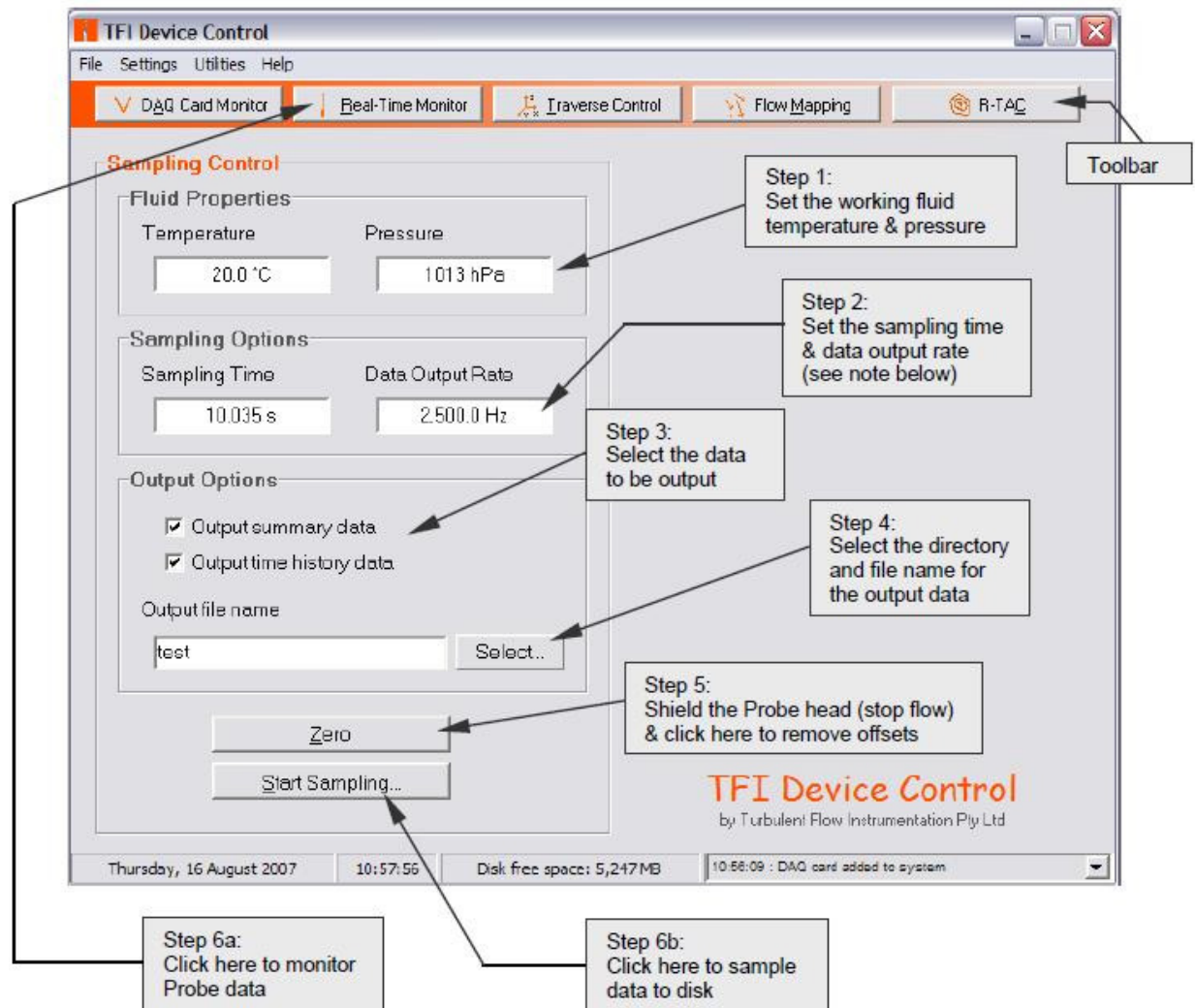


Figure 7-4. Cobra Probe TFI Device Control Data Acquisition Software

Testing Method

The Atmospheric Boundary Layer wind tunnel was tested in the following locations as shown in Figure 7-5. Tests were conducted at the end of each section: fan, plenum, and settling chamber to see the changes in turbulence and mean speed velocities. Tests were conducted at one foot intervals along the test section at both 3 3/8" and 5 3/8" inches from the bottom to ensure that the test section has minimal turbulence and steady flow. Testing was conducted vertically at the end of the test section to estimate the vertical profile of the wind tunnel. Testing was also conducted transversely at the end of the test section to also ensure flow uniformity in the

transverse direction. Finally the first testing location at the beginning of the test section was re-tested for quality control.

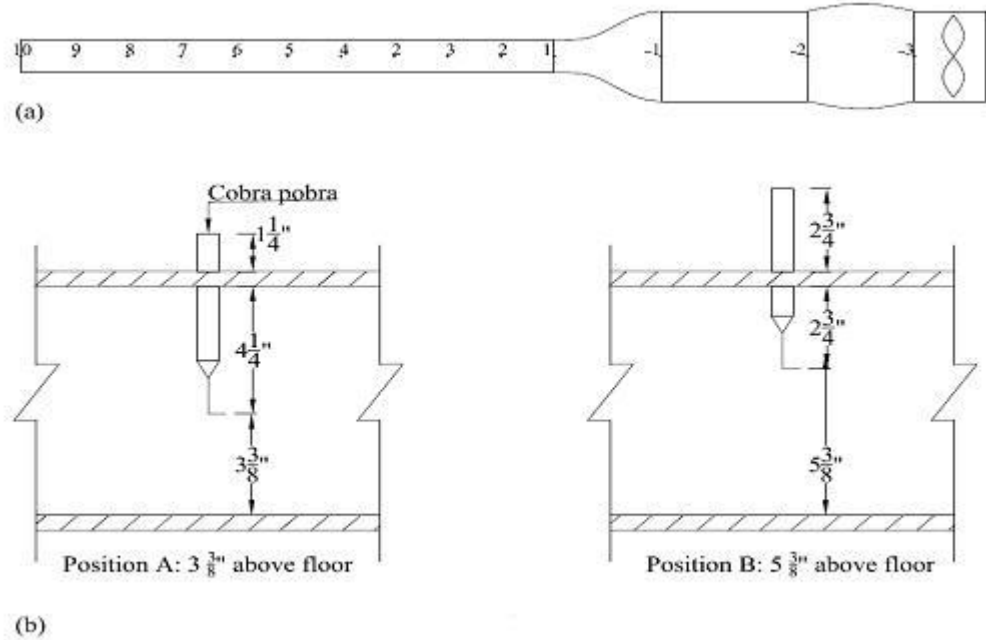


Figure 7-5. ABL Wind Tunnel Testing Locations: A) Longitudinal Locations B) Vertical Locations

To minimize testing irregularities a testing method was established and followed for all the testing locations. After setting up the initial TFI Data Acquisition constraints noted above the following steps were repeated for each testing location:

1. Drill a hole in the wind tunnel at the testing location and duct tape over any previous opening from previous test.
2. Clamp the traverse in place and set it to the appropriate height and location along the wind tunnel using a tape measure (without modifying the grip on the Cobra Probe)
3. Use the infrared gun to input the current wind tunnel temperature into the TFI program.
4. Update the output filename in the TFI software.

5. Click the “Zero” button to re-zero the probe and allow process to completely finish before proceeding to next step.
6. Turn on the fan and allow it to warm-up for approximately 60-90 seconds.
7. Click the “Start Sampling” button and allow the program to finish recording the data.
8. After the program is done recording turn-off the fan and repeat Steps 1-8 until all tests are completed.

Quality Control

Numerous precautions were taken to minimize outside influences. The first and most important quality control method was having two people performing the testing at all times. This limited the number of typographical and testing method errors by having a second pair of eyes reviewing the testing. All the testing was completed the same day using the same Cobra Probe, computer, software, wind tunnel, and setup. In addition, by testing it all on the same day the outside temperature and barometric pressure remained fairly constant. The testing was conducted in an enclosed warehouse with one roll-up door fully opened, this minimized influences of the outside wind while not limiting the airflow around the wind tunnel. The wind tunnel was setup on a table in the center of the warehouse to ensure that there was ample open space for air flow on all sides, in front, and behind the wind tunnel minimizing flow irregularities. The fan was installed on a separate table from the test section minimizing the effect of vibrations on the instrumentation during testing. The testing heights were accurately maintained by using a tape measure for each testing location. The Cobra Probe was calibrated at the manufacture and validated against a hotwire anemometer two weeks earlier. For each test the temperature was updated and the barometric pressure was found using a professional weather station located a few blocks away. A 3 foot tube was used on the Cobra Probe to allow it to read the mean reference pressure away from the wind tunnel's air flow influence. The Cobra Probe was re-

zeroed before each test to minimize changes that may have occurred moving the instrument between test locations. The grip attaching the Cobra Probe to the traverse was kept the same to minimize changes in the rotation of the Cobra Probe relative to the wind tunnel centerline, which could affect the Yaw and Pitch, See Figure 4-2. The fan was turned on for 60-90 seconds before testing to make sure that the fan has achieved its top speed and flow had equalized. The fan was also plugged into its own outlet to minimize voltage variations. Finally, at the end of all the testing the first test location was re-tested and the data correlated with the original output very closely, demonstrating testing precision.

CHAPTER 8

RESULTS AND RECCOMENDATIONS

Results

The complete model ABL wind tunnel testing results can be seen in Table 8-1. Overall results from the model ABL wind tunnel showed relatively constant velocities with minor turbulence.

Testing Locations	X-Location (in)	Y-Location (in)	Number of good samples	Mean temperature (°C)	Barometric pressure (Pa)	Mean reference pressure (Pa)	Mean Flow Speed	Pitch Angle (degrees)	Yaw Angle (degrees)	Pstatic (Pa)	U (m/s)	V (m/s)	W (m/s)	Velocity (m/s)		Turbulence Intensity (%)			
														Min	Max	Overall	Iuu	Ivv	Iww
Position1an	0.00	23.38	204,109 (68.0%)	26.4	102,167.90	0	9.21	-7.4	36.1	178.6	7.16	5.31	-1.32	0	17.8	17.6	17.5	17.9	17.4
Positionplenum	36.00	23.38	70,737 (23.6%)	26.4	102,167.90	0	10.2	-1.3	44.4	171	7.15	7.04	-0.425	2.19	18.8	15.1	12.7	13.6	18.4
Positionsettlingchamber	72.00	21.38	299,959 (100.0%)	25.8	102,167.90	0	4.19	3.5	17.1	139.3	3.97	1.19	0.254	1.37	6.22	9.57	11.9	10.3	5.2
Test Section: 5 3/8" from Bottom																			
Position1t	96.00	5.375	300,032 (100.0%)	23.9	102,167.90	0	14.9	0.9	-13	13.4	14.5	-3.34	0.223	12.2	17.2	3.97	2.14	4.25	4.97
Position2t	108.00	5.375	300,032 (100.0%)	23.9	102,167.90	0	14.7	2.6	-16.7	16.6	14.1	-4.21	0.67	11.2	17.6	3.76	2.5	3.75	4.71
Position3t	120.00	5.375	300,032 (100.0%)	25.6	102,167.90	0	14.8	1.9	-17.2	15.9	14.1	-4.38	0.487	11.9	17.2	3.44	2.48	3.38	4.23
Position4t	132.00	5.375	300,032 (100.0%)	25.6	102,167.90	0	14.9	0.9	-14.2	13.6	14.4	-3.64	0.233	12.3	17.1	3.19	2.45	3.05	3.89
Position5t	144.00	5.375	300,032 (100.0%)	25.6	102,167.90	0	15.1	4.5	-17.8	10.8	14.3	-4.59	1.18	12.6	17.3	2.86	2.34	2.76	3.39
Position6t	156.00	5.375	300,032 (100.0%)	26.1	102,167.90	0	15.4	2.8	-17.3	5.5	14.7	-4.56	0.748	12.8	17.5	2.65	2.22	2.61	3.05
Position7t	168.00	5.375	300,032 (100.0%)	26.1	102,167.90	0	15.5	3.4	-15.7	3.1	14.8	-4.18	0.92	13.2	17.5	2.51	2.23	2.51	2.77
Position8t	180.00	5.375	300,032 (100.0%)	26.1	102,167.90	0	15.7	0.8	-12.7	-1.9	15.3	-3.44	0.229	12.9	17.6	2.43	2.4	2.35	2.54
Position9t	192.00	5.375	300,032 (100.0%)	26.4	102,167.90	0	15.7	3	-17.7	-2.6	14.9	-4.76	0.821	13.1	17.5	2.42	2.53	2.33	2.4
Position10t	204.00	5.375	301,056 (100.0%)	26.4	102,167.90	0	15.7	1.8	-16.3	-3.7	15	-4.4	0.503	3.02	17.6	3.23	4.35	2.63	2.32
Position11tc	216.00	5.375	300,032 (100.0%)	25.8	102,167.90	0	15.4	3.6	-7.6	-1	15.3	-2.05	0.973	12.5	17.5	2.66	3.17	2.51	2.2
Test Section: 5 3/8" from Bottom																			
Position1b	96.00	3.38	300,032 (100.0%)	23.9	102,167.90	0	14.8	3.7	-11.2	16.7	14.4	-2.87	0.939	12	17	3.61	1.89	3.94	4.46
Position2b	108.00	3.38	300,032 (100.0%)	23.9	102,167.90	0	14.8	3.4	-17.3	15.3	14.1	-4.41	0.885	12.1	17.2	3.29	2.15	3.42	4.02
Position3b	120.00	3.38	300,032 (100.0%)	25.6	102,167.90	0	14.9	4.5	-18.3	15.2	14.1	-4.67	1.17	12.2	17.1	3.01	2.22	3.15	3.5
Position4b	132.00	3.38	300,032 (100.0%)	25.6	102,167.90	0	15	1.7	-14.5	12.1	14.5	-3.77	0.441	12.7	17.3	2.83	2.24	2.99	3.16
Position5b	144.00	3.38	300,032 (100.0%)	25.6	102,167.90	0	15.2	4.5	-18	9.4	14.4	-4.68	1.19	12.1	17.5	2.67	2.28	2.76	2.92
Position6b	156.00	3.38	300,032 (100.0%)	26.1	102,167.90	0	15.3	3	-17.4	4.7	14.6	-4.59	0.807	12.1	17.5	2.8	2.79	2.88	2.73
Position7b	168.00	3.38	300,032 (100.0%)	26.1	102,167.90	0	15.3	3.1	-16.5	1.2	14.6	-4.33	0.815	12.1	17.2	3.06	3.37	3.08	2.67
Position8b	180.00	3.38	300,032 (100.0%)	26.1	102,167.90	0	15.4	2.4	-13.3	-2.7	15	-3.53	0.63	11.9	17.6	3.24	3.89	3.04	2.69
Position9b	192.00	3.38	300,032 (100.0%)	26.4	102,167.90	0	15.4	1.3	-17.6	-4.9	14.6	-4.64	0.347	12	17.6	3.41	4.13	3.21	2.74
Position10b	204.00	3.38	300,032 (100.0%)	26.4	102,167.90	0	15.4	2.1	-16.4	-4.7	14.8	-4.34	0.552	12.2	17.6	3.42	4.15	3.28	2.65
Position11bc	216.00	3.38	300,032 (100.0%)	25.8	102,167.90	0	15.1	2.7	-8.1	-1.3	15	-2.13	0.714	11.3	17.4	3.51	4.49	3.15	2.61
Re-test Position																			
Position1b2	96.00	3.38	300,032 (100.0%)	26.4	102,167.90	0	14.7	2.8	-15.1	16.1	14.2	-3.84	0.728	12.5	17.4	3.76	2.02	4.08	4.64
Test Section Vertical Profile																			
Position11bc075	12	0.75	300,032 (100.0%)	25.8	102,167.90	0	12.5	2.2	-8	-2	12.3	-1.74	0.469	7.64	17.6	7.04	9.89	5.67	4.3
Position11bc125	12	1.25	300,032 (100.0%)	25.8	102,167.90	0	13.4	2.4	-10.9	-2.2	13.1	-2.52	0.543	7.95	17.5	6	8.14	5.18	3.88
Position11bc200	12	2.00	303,104 (100.0%)	25.8	102,167.90	0	14.3	0.7	-11.1	-3.1	14	-2.76	0.178	10.1	17.6	4.85	6.35	4.33	3.41
Position11bc	12	3.38	300,032 (100.0%)	25.8	102,167.90	0	15.1	2.7	-8.1	-1.3	15	-2.13	0.714	11.3	17.4	3.51	4.49	3.15	2.61
Position11bc400	12	4.00	300,032 (100.0%)	25.8	102,167.90	0	15.4	1.7	-9.9	-2.7	15.1	-2.66	0.455	12.3	17.4	3.03	3.71	2.82	2.42
Position11tc	12	5.375	300,032 (100.0%)	25.8	102,167.90	0	15.4	3.6	-7.6	-1	15.3	-2.05	0.973	12.5	17.5	2.66	3.17	2.51	2.2
Test Section Horizontal Profile																			
Position11tl	5.25	5.375	300,032 (100.0%)	25.8	102,167.90	0	15.8	3.7	-9.8	-2.1	15.5	-2.68	1.01	12.3	17.4	1.94	2.18	1.9	1.7
Position11tc	12	5.375	300,032 (100.0%)	25.8	102,167.90	0	15.4	3.6	-7.6	-1	15.3	-2.05	0.973	12.5	17.5	2.66	3.17	2.51	2.2
Position11tr	18.75	5.375	300,032 (100.0%)	25.8	102,167.90	0	15.5	-2.4	-7.9	-1.8	15.3	-2.12	-0.657	11.8	17.6	3.15	3.84	3	2.45

Table 8-1. Model ABL Wind tunnel Testing Results

Figure 8-1 shows the mean wind speeds recorded along the test section. The overall wind speed at 3 3/8 inches above the bottom had an average deviation of 0.20 and a mean of 15.15 m/s and followed a generally increasing trend. The X-direction wind speed at 3 3/8 inches above the bottom had a slightly larger standard deviation of 0.23 and a mean of 14.55 m/s following a generally increasing trend. The Y-direction wind speed at 3 3/8 inches above the bottom had a larger standard deviation of 0.67 and a mean of -3.99 m/s, and followed a constant trend. Finally the Z-direction wind speed at 3 3/8 inches above the bottom had a larger standard deviation of 0.21 and a mean of 0.77 m/s, and followed a constant trend.

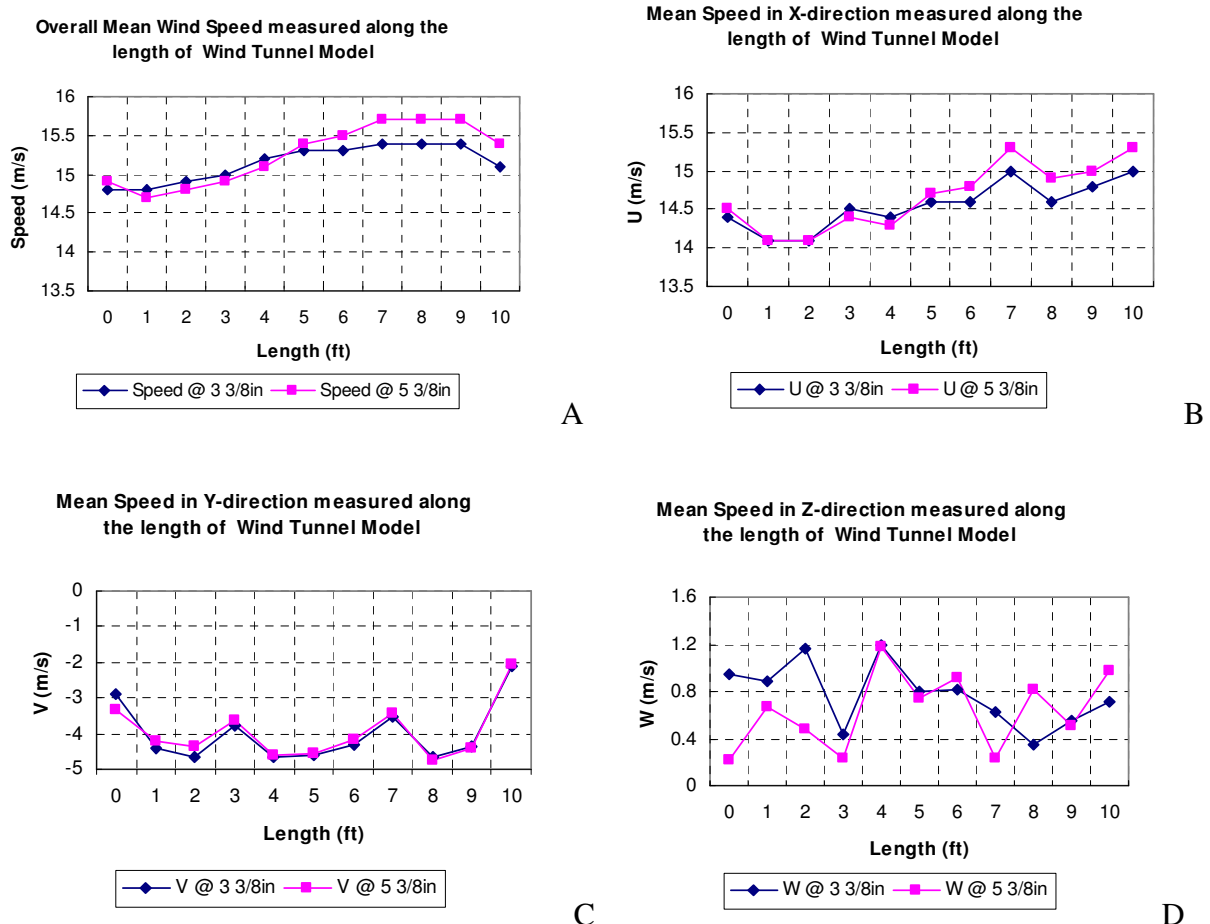
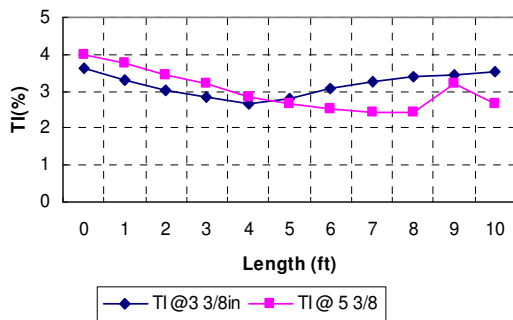


Figure 8-1. ABL Test Section Mean Wind Speed: A) Overall Mean Wind Speed B) Mean Wind Speed in X-Direction C) Mean Wind Speed in Y-Direction D) Mean Wind Speed in Z-Direction

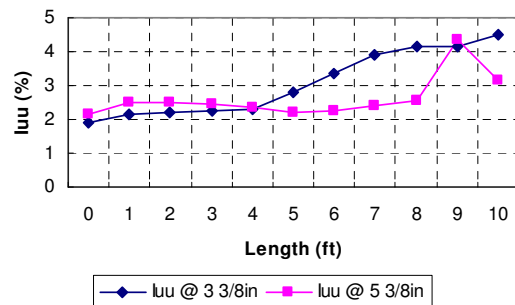
Figure 8-2 shows the mean turbulence intensities recorded along the test section. The overall turbulence intensity at 3 3/8 inches above the bottom had an average deviation of 0.46% and a mean of 3.01% and followed a generally decreasing trend. The longitudinal turbulence intensity at 3 3/8 inches above the bottom had a comparable standard deviation of 0.41% and a mean of 2.62% following a generally increasing trend. The transverse turbulence intensity at 3 3/8 inches above the bottom also had a similar standard deviation of 0.50% and a mean of 2.92%, and followed a negative trend. Finally the vertical turbulence intensity at 3 3/8 inches above the bottom had a larger standard deviation of 0.84% and a mean of 3.32 m/s, and followed a decreasing trend.

Overall Turbulence Intensity measured along the length of Wind Tunnel Model



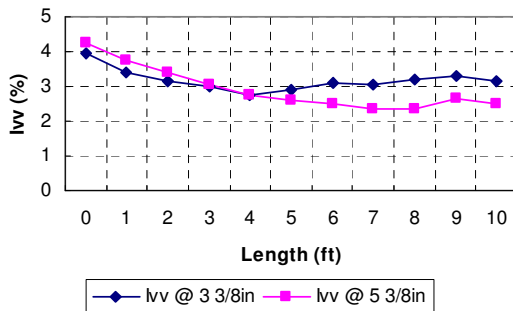
A

Longitudinal Turbulence Intensity measured along the length of Wind Tunnel Model



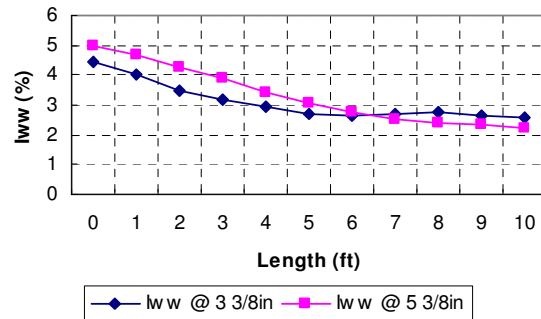
B

Transverse Turbulence Intensity measured along the length of Wind Tunnel Model



C

Vertical Turbulence Intensity measured along the length of Wind Tunnel Model



D

Figure 8-2. ABL Test Section Mean Turbulence: A) Overall Mean Turbulence B) Mean Turbulence in X-Direction C) Mean Turbulence in Y-Direction D) Mean Turbulence in Z-Direction

According to Marshall “turbulence nominal values of 0.5 and + 1 percent have been adopted as performance criteria for intensity of turbulence and velocity non-uniformity, respectively” (Marshall ix). All of these turbulence intensities and mean flow non-uniformities are outside of this range, but are relatively small considering the accuracy of construction and testing. Since the probe was lined up parallel to the centerline of the test section by hand any angle from parallel would affect the relative components in the X and Y directions. That hypothesis seems to be supported by the relative constant nature in the Y-direction plot, and the relatively high negative value – at each location the probe recorded part of the actual X-component of wind speed as Y-component. Since the Z-component is so small those readings are probably because of turbulence or general testing uncertainty. Because of the budget constraints all of the joints were cut by hand, the fifth-order polynomial was cut by hand, and most importantly the honeycomb was constructed on straw at a time by hand, all of which can lead to these relatively small, but significant turbulence and flow non-uniformities values. For the full-size wind tunnel additional mesh screens could be introduced, or even the addition of counter-rotational vanes if the longitudinal turbulence intensity values are still out of range. It can also be seen from Table 4-1 that before the settling chamber the amount of “good” steady data changed from 68% and 28% to 100%, and the overall turbulence intensities dropped from over 17.6% to under 4% demonstrating that the settling chamber is significantly improving the flow quality. It is important to note that the reason why the changes in the transverse and vertical turbulence intensities are not as pronounced as the longitudinal is because the longitudinal turbulence has an “unsteadiness, which can originate from the fan or an intermittent boundary layer separation,

(and) is usually in the form of a low frequency oscillation which mainly contributes to the measured streamwise fluctuation” (Bell and Mehta 3)

Finally, the vertical profile was found by taking readings at various locations at the end of the test section. Figure 8-3 shows the non-dimensional vertical profile of the model ABL wind tunnel.

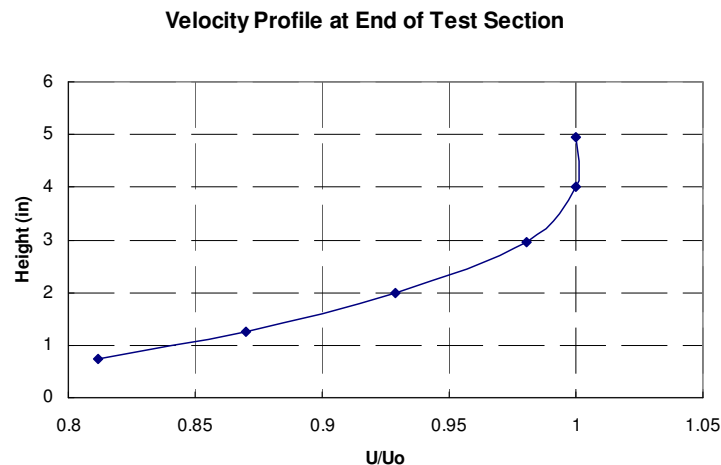


Figure 8-3. ABL Velocity Profile at End of Test Section

Recommendations

There were many problems that came up during the construction of the ABL wind tunnel. All of these problems were solvable by working additional hours, but this significantly pushed back the completion date of the project. The original timeline for the project, which included float time for standard construction problems, was to have the project completed within 12 months by the end of December 2008. Problems with the honeycomb and delivery of materials severely delayed the project making it take over 16 months.

The issue that caused the most problems was the honeycomb. Because of the prohibitive cost of a manufactured metal honeycomb the project was forced to construct one by hand, which took many more hours than anticipated. The first problem was finding an efficient method for

cutting the 35,000+ straws. After trial and error the most efficient method was to bundle approximately 30 straws with a rubber band and cutting the bundle using a guillotine style paper cutter. A template for the length was created by clamping a level at the desired length so that the straws could be pushed flush against it and cut. This however caused the unexpected problem of cold fusing. Because of the large amount of straws and the dulling of the cutting blade the paper cutter would squish the straws together while cutting, causing approximately one out of every five straws to be temporarily joined together. This problem of cold fusing was easily solved by squeezing on the ends of the straws with one's finger tips. Again however this added yet another step and additional time to the honeycomb construction. It was anticipated that during straw placement a very efficient process would be found, but none was. All the methods tested of placing groups of straws and the gluing the together either caused the glue to close the ends of the straws, for the straws not to be parallel, or for the straws not to be completely coated with glue, causing them to break apart for one another when placed in air flow. In the future it would be recommended to first have a much larger budget so that a fabricated honeycomb could be used.

Another issue was to ensure uniform steady flow all of the surfaces and transitions had to flow smoothly. This caused a problem with using screws or bolts, which could penetrate the ABL wind tunnel and lead to irregular flows around the protrusions. The solution to this was to use a combination of rivets, tape, and adhesive to attach the components without any protrusions.

Also to ensure a uniform steady flow the wind tunnel also had to be built within extremely limited tolerances. Without the benefit of machine fabricated pieces that are usually found in wind tunnels additional time and effort was required to keep the dimensions and contraction shapes close to the calculated requirements.

To a lesser degree the anticipated delays with material delivery and items being out of stock also delayed the project. The Patterson fan delivery was held up for over a week because of flooding problems in Tennessee.

One positive recommendation for future projects is that the time spent pre-assembling each section and pre-testing the Cobra Probe saved a significant amount of time. The assembly and testing phases were both completed in three days, much faster than the three weeks originally projected.

Conclusions

In conclusion, the model ABL has been designed using the Open ABL Calculation Worksheet created for this research project. The Open ABL Calculation Worksheet is based on empirical and theoretical equations and serves as a preliminary design for Atmospheric Boundary Layer wind tunnels. The overall design followed general suggestions and requirements stipulated by the literary resources. The wind tunnel was tested using the Cobra Probe from Turbulent Flow Instrumentation. The testing results showed that the turbulence intensities and mean flow non-uniformities were out of the suggested range, and this can mostly be attributed to the budget constraints and the limitations of the empirical and theoretical equations. Overall this project exceeded its original intention of providing a viable ABL wind tunnel design by providing a worksheet that can calculate design parameters for a wide variety of ABL wind tunnels, and by establishing a model wind tunnel that can be used for hurricane research. Using this model ABL wind tunnel and the Open ABL Worksheet future researchers can optimize the wind tunnel design for full-size implementation, someday furthering hurricane research and optimistically saving lives.

LIST OF REFERENCES

- ASCE Aerospace Division Task Committee on Wind Tunnel Studies of Buildings and Structures. "Journal of Aerospace Engineering." Wind-Tunnel Studies of Buildings and Structures 9 (January 1996): 19-36.
- Auld, D. J., and K. Srinivas. "Aerodynamics 4 Students." Google Sites - Free websites and wikis. 1 Apr. 2009. The University of Sydney School of Aerospace, Mechanical and Mechatronic Engineering. 09 Apr. 2009
<<http://sites.google.com/site/aerodynamics4students/>>.
- Barlow, Jewel B., William H. Rae, and Alan Pope. Low-speed wind tunnel testing. 3rd ed. New York: Wiley-Interscience, 1999.
- Barna, P. Stephen. Investigations of Detail Design Issues for the High Speed Acoustic Wind Tunnel Using a 60th Scale Model Tunnel Final Report. [NASA contractor report], NASA CR-191671. Washington, DC: National Aeronautics and Space Administration, 1991.
- Bell, J. H., and R. D. Mehta. Contraction Design for Small Low-Speed Wind Tunnels. [NASA contractor report], NASA CR-177488. Washington, DC: National Aeronautics and Space Administration, 1988.
- Boggs, D. W. "Validation of the Aerodynamic Model Method." Journal of Wind Engineering and Industrial Aerodynamics 41 (1992): 41-44.
- Boyle, M. T., and C. Knaub. "Low speed wind tunnel testing." Semiconductor Thermal and Temperature Measurement Symposium, 1988. SEMI-THERM IV., Fourth Annual IEEE. California, USA, San Diego. 31-39.
- Brassard, Daniel. "Transformation of a Polynomial for a Contraction Wall Profile." Diss. Lakehead University, Ontario, Canada, 2003.

- Clancy, L. J. Aerodynamics. Upper Saddle River: FT Prentice Hall, 1978.
- Cochran, Leighton. Wind Effects on Lowrise Buildings. Tech. Cermak Peterka Petersen Inc. 5 Apr. 2009 <www.cppwind.com/support/papers/papers/structural/lowrisebuildings.pdf>.
- Doolan, Con J. "Numerical Evaluation of Contemporary Low-Speed Wind Tunnel Contraction Designs." Journal of Fluids Engineering 129 (September 2007): 1241-244.
- Hardy, J. E., and T. E. Mc Knight. "Reducing uncertainty in low flows for bench-top wind tunnels." Sensor Review 25 (2005): 46-50.
- Lee, Jeffrey A., and Ted M. Zobeck. "Analysis of velocity profiles from wind tunnel experiments with saltation." ICAR5/GCTE-SEN Joint Conference, International. Proc. of Center for Arid and Semiarid Lands Studies, Texas Tech University, Texas, USA, Lubbock. 2nd ed. Vol. 2. 2002. 10-13.
- Marshall, Richard D., 1985, "Performance Requirements and Preliminary Design of a Boundary Layer Wind Tunnel Facility," National Bureau of Standards U.S. Department of Commerce Rep. No. NBSIR 85-3168.
- Microsoft. "Solver Uses Generalized Reduced Gradient Algorithm." Microsoft Help and Support. 16 Nov. 2006. 8 Apr. 2009 <<http://support.microsoft.com/kb/82890/>>.
- Moonen, Peter, Bert Blocken, Staf Roels, and Jan Carmeliet. "Numerical modeling of the flow conditions in a closed-circuit low-speed wind tunnel." Journal of Wind Engineering and Industrial Aerodynamics 94 (2006): 699-723.
- Rao, Dhanvada M., and Timmy, T. Kariya. The Design and Preliminary Calibration of a Boundary-Layer Flow Channel. Hampton, Va: National Aeronautics and Space Administration, Langley Research Center, 1987.

Patterson Fan Inc. 26" Inch High Velocity Fan Specifications. Brochure. High Velocity Fan Specifications. 13 Feb. 2008. Patterson Fan Inc. 8 Apr. 2009

<http://www.pattersonfan.com/26_INCH.pdf>.

Tomia, and Liftarn. "File:Wind tunnel3-en.svg." Wikimedia Commons. 3 Feb. 2007. Wikimedia Commons. 08 Apr. 2009 <http://commons.wikimedia.org/wiki/File:Wind_tunnel3-en.svg>.

Turbulent Flow Instrumentation Pty Ltd. Getting Started Series 100 Cobra Probe. Brochure. Victoria, Australia, 2008. Technical Support. 1 Oct. 2008. Turbulent Flow Instrumentation. 5 Apr. 2009 <[http://www.turbulentflow.com.au/Downloads/Getting Started - Cobra Probe.pdf](http://www.turbulentflow.com.au/Downloads/Getting_Started_-_Cobra_Probe.pdf)>.

US Census Bureau, "Table 25. Population in Coastal Counties: 1960 to 2006." State and County Quick Facts, 1 Feb. 2008 <www.census.gov/compendia/statab/tables/08s0025.xls>.

The Worthey Connection. "Subsonic Wind Tunnels." The Windtunnel Connection. 23 June 2006. 09 Apr. 2009
<<http://www.worthey.net/windtunnels/subsonic.htm#United%20States%20Department%20of%20Defense%C2%A0>>.

BIOGRAPHICAL SKETCH

I am very interested in geotechnical, hurricane mitigation, and low rise structures. My favorite classes have been Geotechnical Engineering, Hydraulics, and Reinforced Concrete Design, mostly because I really enjoy the upper division classes where you see real world applications of engineering theory. These classes really differentiate what the theory is and how it differs in practice. I have been especially interested in geotechnical areas because of my current job in the Solid Waste Department at Jones Edmunds. Hurricane Research has always been important to me, being born in Louisiana, following the events of Hurricane Katrina further reminds me of the importance of Hurricane research. Hurricane research can help make people around the world living in coastal areas much safer, possibly saving countless lives over the years.